

Port-based teleportation under pure-dephasing decoherence

Rajendra S. Bhati,^{1,*} Michał Studziński,^{2,†} and Jarosław K. Korbicz^{1,‡}

¹*Center for Theoretical Physics, Polish Academy of Sciences,
Aleja Lotników 32/46, 02-668 Warszawa, Poland*

²*International Centre for Theory of Quantum Technologies,
University of Gdańsk, Marii Curie-Skłodowskiej 4, 80-309 Gdańsk, Poland*

(Dated: February 19, 2026)

We study deterministic port-based teleportation in the presence of noise affecting both the entangled resource state and the measurement process. We focus on a physically motivated model in which each Bell pair constituting the resource interacts with an identical local environment, corresponding to independently distributed entangled links. Two noisy scenarios are analysed: one with decoherence acting solely on the resource state and ideal measurements, and another with noisy, noise-adapted measurements optimised for the given noise model. In the first case, we derive an analytical lower bound and later a closed-form expression for the entanglement fidelity of the teleportation channel and analyse its asymptotic behaviour. In the second, we combine semi-analytical and numerical methods. Surprisingly, we find that noise-adapted measurements perform worse than the noiseless ones. To connect the abstract noise description with microscopic physics, we embed the protocol in a spin–boson model and investigate the influence of bath memory and temperature on the teleportation fidelity, highlighting qualitative differences between different environments.

I. INTRODUCTION

Port-based teleportation (PBT), introduced by Ishizaka and Hiroshima [1, 2], is a variant of the standard quantum teleportation protocol [3] in which the receiver applies no unitary correction to the output system. Instead, the sender (Alice) and the receiver (Bob) share a multipartite resource state; Alice performs a single joint measurement on her share of the resource and the input state, and Bob retrieves the teleported state simply by selecting one of his subsystems (ports) according to the classical message sent by Alice. We distinguish two variants of PBT: deterministic non-exact, where the state is always transmitted, but is noisy; probabilistic exact, where if the transmission is successful, then teleportation is perfect. Due to the non-programming theorem [4, 5], both variants cannot be implemented perfectly when the size of the resource state is finite – the teleported state is always noisy, or the probability of failure is always non-zero. Due to this limitation, it was important to understand how the efficiency of the teleportation procedure depends on the dimension of the teleported state, the number of shared ports (size of the resource state), and what the optimal settings of the protocol are. The full answer was given in a series of papers, where the analysis was made possible by the use of tools from representation theory and semidefinite programming [6–10].

Ridding of the unitary correction step in PBT has deep structural implications. This feature endows PBT with a unique operational flexibility that makes it a natural building block for many quantum information tasks – Bob can process the teleported system even before receiving the classical information about which port is correct (delayed input formalism). In this way, PBT underlies a variety of higher-order quantum operations (HOQO) primitives [11], including universal programmable quantum processors [1, 12] and their hybrid versions [13, 14], schemes unitary learning [15], transposing and inverting unitary operations [16–18], as well as protocols for storage and retrieval of unknown operations [19, 20]. Beyond these applications, PBT has also proved influential in more traditional quantum information scenarios, where its structure has enabled progress in instantaneous non-local quantum computation, position-based cryptography [21], and the study of interaction complexity and entanglement in non-local and holographic models [22]. It has further contributed to clarifying the connection between quantum communication complexity advantages and violations of Bell inequalities [23] and others [24–26]. In the last years, progress in the area of PBT has put it on a much firmer mathematical and algorithmic footing: its performance is now fully characterized in terms of representation theory [6, 7, 9, 27], and efficient quantum circuits and algorithms for optimal PBT in various regimes have been constructed [28–30].

All of these developments, however, rely on essentially ideal assumptions: carefully optimized resource state and perfect measurements. In any realistic architecture, the multipartite resource state will be imperfect, affected by local or correlated noise, and the implementation of the PBT measurement itself will suffer from errors. From the operational

* rsbhati@cft.edu.pl

† michał.studzinski@ug.edu.pl; corresponding author

‡ jkorbicz@cft.edu.pl

point of view, a noisy PBT scheme is simply an effective quantum channel acting on the input state; understanding this effective channel is crucial if PBT is to be used as a building block of the above-mentioned primitives. Studying PBT in noisy conditions is therefore not merely a technical refinement of the ideal theory, but a necessary step in assessing its true operational power. This direction is beginning to be explored: for instance, recent work [31] has analyzed PBT when the shared ports are subjected to local Pauli noise, fully characterizing the induced teleportation channel, and using this to study port-based entanglement teleportation as a tool for entanglement distribution in quantum networks.

Motivated by these developments, we study PBT in an open-quantum-systems setting. Rather than treating noise only at the level of an effective teleportation channel, we explicitly model the interaction between each entangled resource pair and its environment, allowing us to derive the resulting noisy PBT channel from the underlying dynamics. In particular:

- (a) We focus on the deterministic PBT, where each Bell pair forming the resource state is coupled to its own local environment, with all environments assumed to be identical, reflecting a scenario in which the parties share N identical entangled ‘wires’. While more general models with a common environment are possible, they are technically more involved and are not considered here, except for a simple commuting subcase. The used model is discussed in more detail in Section III.
- (b) We consider two scenarios of the noisy PBT protocol. In the first one we have a noisy resource state and noiseless measurement, where we assume perfect control over the measurements in Alice’s laboratory, and uncontrolled interaction of the resource state distributed among the parties. In this scenario, we first derive a lower bound for the entanglement fidelity of the teleportation channel using techniques introduced in [21]. Then we develop a fully analytical approach to the problem, presenting a closed-form expression for the entanglement fidelity, together with a discussion on its asymptotic behaviour. This is contained in Section IV and Section V. In the second case, we assume a scenario with noisy measurements. In particular, our measurements are noise-adapted ones, meaning our goal is to provide the best possible measurement set for a given noisy scenario. Here, we mostly rely on a semi-analytical approach, supported strongly by a numerical approach. However, for the special case of $N = 2$, we derive a fully analytical lower bound on the entanglement fidelity relying on Helstrom’s bound. This is considered in Section VI.
- (c) In order to illustrate the impact of realistic environments, on the performance of the noisy PBT protocol, we apply our general results to the concrete example of the spin–boson model [32–34], which has been widely used to model interactions of physical qubits with their environments, see e.g. [35–38] and references therein. The model describes a central spin-register, in our case two spins of each of the Bell pair, interacting with a thermal bosonic bath. The model is parametrized in terms of three dimensionless quantities: the Ohmicity exponent s , the ratio of the thermal energy to the cutoff energy T/Λ , and the dimensionless time $\tau = t\Lambda$ (we are using units in which $\hbar = 1$ for simplicity). We illustrate the impact of microscopic noise properties by analysing two representative environmental regimes: modelled by a super-Ohmic spectral density with $s = 2$, which for a single qubit corresponds to a Markovian regime with weak memory effects, and with $s = 3$, corresponding to a non-Markovian regime with enhanced environmental memory. In both cases, we study the time dependence of the teleportation fidelity as a function of time to show how the duration of the decoherence affects the teleportation process. This is considered in Section VII.

The whole paper contains additionally Section II, where all preliminary informations are collected, and several Appendices (Appendix A-G), where for the Reader’s convenience, we collect all detailed calculations and proofs.

II. PRELIMINARY INFORMATIONS AND THE DETERMINISTIC NOISELESS PBT

In this section, we collect all the necessary information about the quantities that measure the efficiency of the deterministic PBT, as well as present information on the deterministic PBT itself, which is necessary to follow the technicalities presented throughout the manuscript. For more details, we refer the reader to previous works.

We start from the basic definitions of the average fidelity and entanglement fidelity. The average fidelity of a quantum channel \mathcal{C} (here teleportation channel) is given by

$$f(\mathcal{C}) := \int \langle \psi | \mathcal{C}(|\psi\rangle\langle\psi|) | \psi \rangle d\psi, \quad (1)$$

where the integral is performed with respect to the uniform distribution $d\psi$ over all d -dimensional pure states [39].

The entanglement fidelity of a channel \mathcal{C} is given by

$$F(\mathcal{C}) := \text{Tr}[P^+ (\mathcal{C} \otimes \mathbf{1}) P^+], \quad \text{where} \quad P^+ := \frac{1}{d} \sum_{i,j=1}^d |i\rangle\langle j| \otimes |i\rangle\langle j| \quad (2)$$

is the projector on the bipartite maximally entangled state $|\psi^+\rangle = (1/\sqrt{d}) \sum_i |ii\rangle$, and $\mathbf{1}$ denotes the identity channel. There is a universal relation between the teleportation fidelity f and entanglement fidelity F [39] expressed by

$$f(\mathcal{C}) = \frac{2F(\mathcal{C}) + 1}{3}. \quad (3)$$

In this paper, we consider the standard PBT scheme first proposed in [1], and restrict our discussion to qubit systems, i.e., when $d = 2$. In the standard configuration of any PBT protocol, the sender (Alice) and the receiver (Bob) share a $2N$ -qubit pure state (resource state):

$$\Psi_{\vec{A}\vec{B}}^- := \psi_{A_1 B_1}^- \otimes \cdots \otimes \psi_{A_N B_N}^-, \quad (4)$$

where $\vec{A} = A_1 A_2 \cdots A_N$, $\vec{B} = B_1 B_2 \cdots B_N$, and $P_{A_i B_i}^- \equiv \psi_{A_i B_i}^- := |\psi^-\rangle\langle\psi^-|_{A_i B_i}$ is the projector on the bipartite singlet state of two qubits on the i -th port:

$$|\psi^-\rangle_{A_i B_i} := \frac{1}{\sqrt{2}}(|01\rangle - |10\rangle). \quad (5)$$

Alice teleports an unknown qubit state ρ_C by performing a joint POVM measurement $\{\Pi_i\}_{i=1}^N$ on the systems \vec{A} and C , yielding an outcome $i \in \{1, \dots, N\}$. After the measurement, she sends her outcome i to Bob using a classical communication channel. Bob, to recover the teleported state, selects qubit B_i , and removes the rest of his qubits. The PBT channel is expressed as

$$\mathcal{C}(\rho_C) := \sum_{i=1}^N \text{tr}_{\vec{A}\vec{B}_i C} \left[(\Pi_i^{\vec{A}C} \otimes \mathbf{1}_{\vec{B}}) (\Psi_{\vec{A}\vec{B}}^- \otimes \rho_C) \right]_{B_i \rightarrow B}, \quad (6)$$

where $\text{tr}_{\vec{B}_i}$ denotes tracing out all systems but B_i . The selected port is regarded as a common qubit B with the teleported state, which is just a renaming, denoted by $B_i \rightarrow B$. Since we work with deterministic and non-exact transmission to quantify performance of the teleportation channel, we use the entanglement fidelity $F(\mathcal{C})$ from (2), but for P^- instead of P^+ . It is because the entanglement fidelity is invariant under local unitaries, and the considered states are connected by a unitary of the form $Y \otimes \mathbf{1}$, where $Y = \begin{pmatrix} 0 & -i \\ i & 0 \end{pmatrix}$ is a Pauli matrix. The exact form of the entanglement fidelity $F(\mathcal{C})$ for the teleportation channel \mathcal{C} is given by [1, 2]:

$$F(\mathcal{C}) = \frac{1}{2^{N+3}} \sum_{k=0}^N \left(\frac{N-2k-1}{\sqrt{k+1}} + \frac{N-2k+1}{\sqrt{N-k+1}} \right)^2 \binom{N}{k}. \quad (7)$$

For further purposes, we present derivations of the above expression in Appendix D. In the asymptotic limit $N \rightarrow \infty$, the entanglement fidelity and the average fidelity behave respectively as: behaves as:

$$F(\mathcal{C}) \rightarrow 1 - \frac{3}{4N}, \quad f(\mathcal{C}) \rightarrow 1 - \frac{1}{2N}. \quad (8)$$

The asymptotic of the deterministic and probabilistic PBT is also known for the case when $d > 2$ and presented in papers [6, 9]. The maximal value of the entanglement fidelity from (2) is achieved by so-called square-root measurement (SRM) or, equivalently, pretty bad measurements (PBM). These measurements have the following explicit form for every $1 \leq i \leq N$:

$$\Pi_i := \tilde{\Pi}_i + \Delta, \quad \Delta := \frac{1}{N} \sum_{i=1}^N \tilde{\Pi}_i, \quad (9)$$

with

$$\tilde{\Pi}_i^{\vec{A}C} := \rho^{-1/2} \sigma_i \rho^{-1/2}, \quad \rho := \sum_{i=1}^N \sigma_i. \quad (10)$$

The operators σ_i are called signal states, expressed as

$$\sigma_i := \frac{1}{2^{N-1}} \psi_{A_i C}^- \otimes \mathbf{1}_{\bar{A}_i}, \quad (11)$$

where $\mathbf{1}_{\bar{A}_i}$ represents the identity operator acting on all \bar{A} systems excluding system A_i . The inverse in (10) is taken on the support of ρ and thus the POVM must be supplemented by the operator Δ to have $\sum_i \Pi_i^{\bar{A}C} = \mathbf{1}_{\bar{A}C}$, which projects on the zero-eigenvalue subspace and thus has no contribution to the entanglement fidelity. The explicit proof of optimality of the SRM measurements for the deterministic PBT has been shown in [10].

III. THE NOISY TELEPORTATION CHANNEL

In this work, we will assume that the environment affects the Bell pairs only, while the qubit, which state we are about to teleport stays unaffected. This is an approximation to a real situation, motivated by the fact that entangled states decohere faster than the states of a single system [40–43]. We will assume the following form of the interaction between the Bell pairs AB and the environment E :

$$H_{int} = \sum_{i,j \in \{0,1\}} |ij\rangle\langle ij|_{AB} \otimes V_{ij}^E, \quad (12)$$

which has the form of a general pure dephasing in the product basis $|ij\rangle = |i\rangle \otimes |j\rangle$ of the qubits AB , i.e. it destroys coherence in the basis $|ij\rangle$, in particular it decoheres Bell states. The basis $\{|ij\rangle\}$ is called the pointer basis and without a loss of generality we can choose it to be the eigenbasis of σ_z . The environmental coupling observables V_{ij}^E are at this point left arbitrary. The form of the interaction (12) is motivated by physical considerations as it is often encountered in open systems. For example, a broad class of dynamics of a type $H = S_A \otimes V_E + S_B \otimes V'_E + H_E$, where $S_{A,B}$ are the coupling observables of the systems A and B side, V_E, V'_E the corresponding environmental coupling observables and the H_E internal dynamics of the environment can be transformed to form (12). The internal dynamics of the qubits is assumed to be suppressed or at most commuting with the interaction $[H_{AB}, S_A] = [H_{AB}, S_B] = 0$. Although this can be criticized from the open system's perspective as a rather restrictive condition, it can be nevertheless justified here as one would like to prepare the communication qubits as close to the Bell state as possible and keep them in that state. Another reason for this choice is the fact that it allows for analytical calculations in principle without the need of the tracing out of the environment, which may be kept as a bona fide quantum system throughout the analysis. This in turn may reveal surprising decoherence suppression effects like e.g. the purifying teleportation [44]. Although we will not study such scenarios here due to their complication in the case of the PBT scheme, our approach can be in principle directly applied to it in the future. A concrete example of the dynamics (12) is the popular spin-boson model with multiple spins (a spin register) [32–34, 45], which we will study in Section VII.

The Hamiltonian (12) generates the following unitary evolution, known as pure dephasing evolution in the open systems community, coherent control or generalized C-NOT evolution in the quantum information community, or generalized von Neumann measurement in the measurement theory:

$$U_{AB:E} = \sum_{i,j \in \{0,1\}} |ij\rangle\langle ij| \otimes \exp(-iV_{ij}t). \quad (13)$$

The state of any of the Bell pairs after the decoherence is given by

$$\tilde{P}_{AB}^- = \text{tr}_E U_{AB:E} (|\Psi^-\rangle\langle\Psi^-|_{AB} \otimes \rho_E) U_{AB:E}^\dagger \quad (14)$$

$$= \frac{1 + |\Gamma| \cos \theta}{2} |\Psi^-\rangle\langle\Psi^-| + \frac{1 - |\Gamma| \cos \theta}{2} |\Psi^+\rangle\langle\Psi^+| + \frac{i|\Gamma| \sin \theta}{2} (|\Psi^+\rangle\langle\Psi^-| - |\Psi^-\rangle\langle\Psi^+|) \quad (15)$$

$$= \frac{1 + |\Gamma|}{2} \mathbf{1} \otimes R(\theta) |\Psi^-\rangle\langle\Psi^-|_{AB} \mathbf{1} \otimes R(\theta)^\dagger + \frac{1 - |\Gamma|}{2} \mathbf{1} \otimes R(\theta) \sigma_z |\Psi^-\rangle\langle\Psi^-|_{AB} \mathbf{1} \otimes \sigma_z R(\theta)^\dagger \quad (16)$$

$$\equiv \mathbf{1} \otimes \mathcal{E}_\Gamma (|\Psi^-\rangle\langle\Psi^-|_{AB}). \quad (17)$$

Here

$$\Gamma = \text{tr}_E [e^{-iV_{01}t} \rho_E e^{iV_{10}t}] \equiv |\Gamma| e^{i\theta}, \quad (18)$$

$|\Gamma| \leq 1$, is the only non-trivial decoherence factor, $R(\theta)$ is a relative phase rotation in the pointer basis:

$$R(\theta) = e^{-i\theta} |0\rangle\langle 0| + |1\rangle\langle 1|, \quad (19)$$

and \mathcal{E}_Γ is a single qubit decoherence channel, defined as:

$$\mathcal{E}_\Gamma(\rho) = R(\theta) \left[\frac{1 + |\Gamma|}{2} \rho + \frac{1 - |\Gamma|}{2} \sigma_z \rho \sigma_z \right] R(\theta)^\dagger. \quad (20)$$

The high symmetry of $|\Psi^-\rangle$ allows to move the effect of the environment to a single qubit only, despite the correlated character of the interaction (12). If the decoherence factor was real, i.e. $\theta = 0$, this would be a Pauli noise channel with operators $\mathbb{1}, Z$ [31]. The decoherence factor (18) depends on the interaction time t , but for the moment we neglect that dependence and study the efficiency of the protocol as a function of Γ . We note that $\Gamma = 1$ corresponds to no decoherence, while $\Gamma = 0$ to a fully decohered, separable resource, which is no different from using classical randomness:

$$\tilde{P}_{AB}^-(\Gamma = 0) = \frac{1}{2} |01\rangle\langle 01| + \frac{1}{2} |10\rangle\langle 10|. \quad (21)$$

Let us now briefly describe the PBT procedure [1, 2, 31]. Consider that Alice and Bob share N singlet pairs, which were affected by the decoherence (20). The shared resource state becomes:

$$\rho_{\vec{A}\vec{B}} = \bigotimes_{i=1}^N |\Psi^-\rangle\langle \Psi^-|_{A_i B_i} \equiv \bigotimes_{i=1}^N \tilde{P}_{A_i B_i}^-, \quad (22)$$

where Alice and Bob have N qubits each A_1, A_2, \dots, A_N and B_1, B_2, \dots, B_N , respectively. Here onwards, we use the following notations through out the paper: Alice's N qubits are denoted by \vec{A} , all except A_i is denoted by \bar{A}_i , all except A_i and A_j are denoted by \bar{A}_{ij} , and so on. Similar notations are adopted for Bob's qubits as well. The resource state $\rho_{\vec{A}\vec{B}}$ is employed for teleportation of an unknown state of another qubit, say C , from A to B . Alice performs a joint measurement with N possible outcomes on the \vec{A} and C qubits, described by a POVM $\{\Pi_i\}$. Alice then sends the information regarding the index of the outcome, for example the i -th outcome, and Bob selects the corresponding port and discards the rest. The selected port is regarded as a common qubit B with the teleported state, which is just a renaming, denoted by $B_i \rightarrow B$. The corresponding teleportation channel, which maps the state acting on the Hilbert space \mathcal{H}_C to those on \mathcal{H}_B and assuming corrupted resource (14) then reads (cf. [31]):

$$\mathcal{C}(\sigma_C^{in}) = \sum_{i=1}^N \left[\text{tr}_{\vec{A}\bar{B}_i C} \sqrt{\Pi_i} (\rho_{\vec{A}\vec{B}} \otimes \sigma_C^{in}) \sqrt{\Pi_i}^\dagger \right]_{B_i \rightarrow B} = \sum_{i=1}^N \text{tr}_{\vec{A}C} \Pi_i \left[\eta_{\vec{A}B}^{(i)} \otimes \sigma_C^{in} \right], \quad (23)$$

where we introduced the following, normalized, states:

$$\eta_{\vec{A}B}^{(i)} = [\text{tr}_{\bar{B}_i} (\rho_{\vec{A}\vec{B}})]_{B_i \rightarrow B} = \frac{1}{2^{N-1}} \tilde{P}_{A_i B}^- \otimes \mathbb{1}_{\bar{A}_i} \quad (24)$$

The state $\eta_{\vec{A}B}^{(i)}$ can be expressed as a mixture of signal states corresponding to the scenarios when a noiseless PBT is performed with $|\Psi^-\rangle^{\otimes N}$ and $|\Psi^+\rangle^{\otimes N}$ states as the resources and a subsequent phase rotation at the Bob's qubit:

$$\eta_{\vec{A}B}^{(i)} = R(\theta)_B \left[\frac{1 + |\Gamma|}{2} \sigma_{\vec{A}B}^{(i)} + \frac{1 - |\Gamma|}{2} \omega_{\vec{A}B}^{(i)} \right] R(\theta)_B^\dagger, \quad (25)$$

where:

$$\sigma_{\vec{A}B}^{(i)} = \frac{1}{2^{N-1}} |\Psi^-\rangle\langle \Psi^-|_{A_i B} \otimes \mathbb{1}_{\bar{A}_i}, \quad (26)$$

$$\omega_{\vec{A}B}^{(i)} = \frac{1}{2^{N-1}} |\Psi^+\rangle\langle \Psi^+|_{A_i B} \otimes \mathbb{1}_{\bar{A}_i}. \quad (27)$$

The entanglement fidelity F of \mathcal{C} is given by:

$$F = \text{tr} P_{BD}^- [(\mathcal{C} \otimes \mathbb{1}) P_{CD}^-] = \text{tr} \sum_{i=1}^N P_{BD}^- \Pi_i^{\vec{A}B} \left\{ \eta_{\vec{A}B}^{(i)} \otimes P_{CD}^- \right\} = \frac{1}{2^2} \sum_{i=1}^N \text{tr} \Pi_i^{\vec{A}B} \eta_{\vec{A}B}^{(i)} \equiv \frac{N}{4} P_{succ}. \quad (28)$$

As the last equality above shows, it is proportional to the success probability of the state discrimination task defined by the ensemble $\left\{ \frac{1}{N}, \eta_{\vec{A}B}^{(i)} \right\}_{i=1}^N$, $i = 1, 2, \dots, N$, of equiprobable signal states $\eta_{\vec{A}B}^{(i)}$ of (24). The problem of finding the

teleportation fidelity then reduces to the state discrimination task, as in the original PBT protocol. Following the original idea [1, 2], we will use the, so called, pretty good measurement (PGM) [10, 21] as a standard tool for state discrimination tasks. It is defined for an ensemble $\{p_i, \sigma_i\}_{i=1}^N$ as:

$$\Pi_i \equiv p_i \bar{\sigma}^{-1/2} \sigma_i \bar{\sigma}^{-1/2}, \quad (29)$$

where $\bar{\sigma} \equiv \sum_i p_i \sigma_i$ is the ensemble average state and if it has zero eigenvalues, the inverse is taken on the support of σ and the POVM is supplemented by the operator $\Delta \equiv \mathbb{1} - \sum_i \Pi_i$, which projects on the zero-eigenvalue subspace and thus has no contribution to the success probability.

However, the states (24) to be discriminated are now more complicated than in the original PBT scheme, i.e. for $\Gamma = 1$. First, their non-trivial part, the reduction to the $A_i B$ subspace is not pure but mixed, supported on a $2D$ subspace spanned by $|\Psi^-\rangle, |\Psi^+\rangle$, cf. (16). Second, and more importantly, the original symmetry $U^{\otimes N} \otimes YU^*Y$ of the non-decohered ensemble $\{\sigma_{AB}^{(i)}\}$ (26) is lost. The latter allowed for a great simplification: using the spin representation theory, the authors of [1, 2] were able to simultaneously diagonalize the ensemble states, their average, and the pretty good measurement $\{\Pi_i\}$ and as a result calculate the fidelity analytically. Under the action of decoherence, the unitary symmetry is lost since $|\Psi^+\rangle$ has a different symmetry than $|\Psi^-\rangle$: $|\Psi^+\rangle = U \otimes XU^*X |\Psi^+\rangle$ and although each ensemble state (24) will still have the $U^{\otimes(N-1)}$ symmetry, their average will not inherit it as the part $\mathbb{1}_{\bar{A}_i}$ is supported on a different subspace for each i .

As a remark, we note that one would be tempted to use the Knill-Barnum bound [46–48] to estimate P_{succ} as in fact the former was derived with the help of the PGM. The bound reads $P_{succ} \geq 1 - \sum_{i \neq j} \sqrt{p_i p_j} F(\sigma_i, \sigma_j)$, where $F(\sigma_i, \sigma_j) \equiv \text{tr} \sqrt{\sqrt{\sigma_i} \sigma_j \sqrt{\sigma_i}}$ the pairwise state fidelity of the ensemble. In our case, we obtain from (24), see Appendix A

$$F(\eta^{(i)}, \eta^{(j)}) = \frac{1}{2} \quad (30)$$

which is both N - and Γ -independent and leads to a bound $P_{succ} \geq 1 - \frac{1}{N} \frac{N(N-1)}{4} = 1 - \frac{N-1}{4}$, which trivializes already for $N > 3$.

Below, we analyse three better strategies, of increasing complication, for estimating the PBT efficiency under the pure dephasing decoherence.

IV. THE BEIGI-KÖNIG BOUND

The easiest way to obtain a bound on the fidelity (28) is to use the main result of [21]: The success probability of the PGM for the equiprobable ensemble $\{\frac{1}{N}, \eta^{(i)}\}_{i=1}^N$ is bounded by:

$$P_{succ}^{pgm} \geq \frac{1}{N \bar{r} \text{tr} \bar{\eta}^2}, \quad (31)$$

where $\bar{\eta} = (1/N) \sum_{i=1}^N \eta^{(i)}$ is the ensemble average state, $\text{tr} \bar{\eta}^2$ is its purity, and $\bar{r} = (1/N) \sum_{i=1}^N \text{rank} \eta^{(i)}$ is the average rank. From (24) we obtain:

$$\text{tr} \bar{\eta}^2 = \frac{1}{2^N N} \left(|\Gamma|^2 + \frac{N+1}{2} \right). \quad (32)$$

where we have used the individual state purities:

$$\text{tr}[(\eta^{(i)})^2] = \frac{1}{2^{N-1}} \text{tr}(\tilde{P}^-)^2 = \frac{1 + |\Gamma|^2}{2^N}, \quad (33)$$

and $\text{tr}\{\eta^{(i)} \eta^{(j)}\}_{i \neq j} = 2^{-(N+1)}$. Since $\text{rank} \eta^{(i)} = 2^{N-1} \cdot \text{rank} \tilde{P}^- = 2^N$ for every i , cf. (24), we obtain:

$$P_{succ}^{pgm} = \frac{2}{N} \left(1 + \frac{1 + 2|\Gamma|^2}{N} \right)^{-1} \geq \frac{2}{N} \left(1 - \frac{1 + 2|\Gamma|^2}{N} \right), \quad (34)$$

and from this the bound on the entanglement fidelity:

$$F \geq \frac{1}{2} \left(1 - \frac{1 + 2|\Gamma|^2}{N} \right). \quad (35)$$

This formula looks almost correct in the absence of decoherence, $\Gamma = 1$, apart that the bound is one half of what it should be [21]. This is the consequence of the fact that above rank $\tilde{P}^- = 2$, while for the ideal, uncorrupted resource obviously rank $P^- = 1$. The bound (35) experiences a drop whenever the rank of the signal states increases. We thus conclude that (35) is of very limited use here as gives half of the expected entanglement fidelity even for very small decoherence effects.

V. PBT USING THE NOISELESS ISHIZAKA-HIROSHIMA MEASUREMENTS

The next strategy is to use the original Ishizaka-Hiroshima deterministic PGM, constructed from the noiseless ensemble, i.e. from $\eta_{\vec{A}B}^{(i)}$ with $\Gamma = 1$, cf. [31]. We will call it the noiseless measurement and its elements the noiseless POVM's. The motivation is that one can imagine a situation, where the noise estimation, i.e. the estimation of Γ , is impossible or even if possible, it cannot be used to fine-tune the measurements. The natural choice is then to use the noiseless measurement as at least for weak decoherence it will perform close to optimal. As we will show, this strategy performs surprisingly well not only for the weak decoherence.

There are at least two possible approaches: A direct calculation of the entanglement fidelity (28) or a calculation using the fact that the PBT channel (23) is a depolarizing channel for noiseless measurements [1, 2]. The latter was studied in [31] and here we perform a direct calculation for completeness, presenting below only the main steps while the detailed calculations can be found in the Appendix B.

For simplicity, throughout this Section we will use the un-normalized ensemble average and POVMS, i.e. we consider the ensemble $\left\{ \frac{1}{N}, \sigma_{\vec{A}B}^{(i)} \right\}$, with $\sigma_{\vec{A}B}^{(i)}$ given by (26), and define the un-normalized average state by:

$$\rho = \sum_{i=1}^N \sigma_{\vec{A}B}^{(i)}, \quad (36)$$

where we used the ρ rather than $\bar{\sigma}$ to comply with the original notation of [1, 2]. As it turns out, the original analysis based on the symmetry and the spin decomposition can be still applied here with a slight modification.

Since all the $\sigma_{\vec{A}B}^{(i)}$ share the same symmetry, the average state (36) shares it also and can be shown to be block-diagonal with respect to the total spin s of the system of $(N+1)$ spins 1/2, given by the qubits $\vec{A}B$:

$$\rho = \sum_{s=s_{min}}^{(N-1)/2} \rho_-(s) \oplus \rho_+(s), \quad (37)$$

where $s_{min} = 0$ for N even and 1/2 for N odd; $\rho_-(s)$ and $\rho_+(s)$ are two families of the block states expressed in terms of eigenstates of ρ as:

$$\rho_{\mp}(s) = \lambda_{s\mp 1/2}^{\mp} \sum_{m=-s}^s \left[\sum_{\beta} \left| \Psi_I(\lambda_{s\mp 1/2}^{\mp}; m, \beta) \right\rangle \left\langle \Psi_I(\lambda_{s\mp 1/2}^{\mp}; m, \beta) \right| + \sum_{\beta} \left| \Psi_{II}(\lambda_{s\mp 1/2}^{\mp}; m, \beta) \right\rangle \left\langle \Psi_{II}(\lambda_{s\mp 1/2}^{\mp}; m, \beta) \right| \right], \quad (38)$$

where

$$\rho \left| \Psi_{I(II)}(\lambda_{s\mp 1/2}^{\mp}; m, \beta) \right\rangle = \lambda_{s\mp 1/2}^{\mp} \left| \Psi_{I(II)}(\lambda_{s\mp 1/2}^{\mp}; m, \beta) \right\rangle, \quad (39)$$

and the above states are explicitly written in Appendix B. The spin index s is there implicitly, $m = -s \dots s$ is the usual magnetic number for spin s , and the index beta β corresponds to the irrep multiplicity and characterizes degeneracy of the corresponding eigenvalues: For $\lambda_{s-1/2}^-$ the degeneracy is $g^{[N-1]}(s)$ and $g^{[N-1]}(s-1)$ for the eigenstates $\left| \Psi_I(\lambda_{s-1/2}^-; m, \beta) \right\rangle$ and $\left| \Psi_{II}(\lambda_{s-1/2}^-; m, \beta) \right\rangle$, respectively. Similarly, the degeneracy of $\lambda_{s+1/2}^+$ is $g^{[N-1]}(s+1)$ and $g^{[N-1]}(s)$ for the eigenstates $\left| \Psi_I(\lambda_{s+1/2}^+; m, \beta) \right\rangle$ and $\left| \Psi_{II}(\lambda_{s+1/2}^+; m, \beta) \right\rangle$, respectively, where

$$g^{[N]}(s) = \frac{N!(2s+1)}{(N/2-s)!(N/2+1+s)!}. \quad (40)$$

The noiseless POVM's can be now constructed from ρ as:

$$\forall_{1 \leq i \leq N} \quad \Pi_i = \rho^{-1/2} \sigma_{\vec{A}B}^{(i)} \rho^{-1/2}, \quad (41)$$

where we have dropped the $1/N$ normalization factor and the inverse is on the support of ρ . Using (15) and (24), we can write down the success probability of detecting the noisy state $\eta_{\vec{A}B}^{(i)}$ by the noiseless POVM defined above. This is the main object of study in this Section:

$$\forall_{1 \leq i \leq N} \quad \text{tr} \Pi_{\vec{A}B}^{(i)} \eta_{\vec{A}B}^{(i)} = \frac{1 + |\Gamma| \cos \theta}{2} \text{tr} \Pi_{\vec{A}B}^{(i)} \sigma_{\vec{A}B}^{(i)} + \frac{1 - |\Gamma| \cos \theta}{2} \text{tr} \Pi_{\vec{A}B}^{(i)} \omega_{\vec{A}B}^{(i)} \quad (42)$$

$$+ \frac{i|\Gamma| \sin \theta}{2} \text{tr} \Pi_{\vec{A}B}^{(i)} \left[(|\Psi^+\rangle\langle\Psi^-| - |\Psi^-\rangle\langle\Psi^+|)_{A_i B} \otimes \frac{\mathbf{1}_{\vec{A}_i}}{2^{N-1}} \right] \quad (43)$$

The first term above is the original Ishizaka-Hiroshima, calculated in [1, 2]. The second term differs in that instead of $|\Psi^-\rangle$, the ensemble states are constructed using $|\Psi^+\rangle$, cf. (27), and the last term is a mixed term. This allows to easily diagonalize all the operators in (42). Building on the original works, let us introduce two families of states:

$$\forall_{1 \leq i \leq N} \quad \left| \xi_{\mp}^{(i)}(s, m, \beta) \right\rangle = \left| \Psi^{\mp} \right\rangle_{A_i B} \left| \Phi^{[N-1]}(s, m, \beta) \right\rangle_{\vec{A}_i}, \quad (44)$$

where $\left| \Phi^{[N-1]}(s, m, \beta) \right\rangle_{\vec{A}_i}$ are appropriately chosen basis states in the space of $N - 1$ qubits. States $\left| \xi_{\pm}^{(i)}(s, m, \beta) \right\rangle$ were shown to diagonalize $\sigma_{\vec{A}B}^{(i)}$ [1, 2], and by the same argument states $\left| \xi_{+}^{(i)}(s, m, \beta) \right\rangle$ diagonalize $\omega_{\vec{A}B}^{(i)}$. We note that $\left| \xi_{+}^{(i)}(s, m, \beta) \right\rangle$ vectors are just the σ_z rotated Ishizaka-Hiroshima vectors, where the rotation can be conveniently applied to the qubit B : $\left| \xi_{+}^{(i)}(s, m, \beta) \right\rangle = \sigma_z^B \left| \xi_{+}^{(i)}(s, m, \beta) \right\rangle$, cf. (16). To complete the calculation, we need the following overlaps, which can be calculated for every $1 \leq i \leq N$:

$$\left\langle \xi_{+}^{(i)}(s, m, \beta) \middle| \Psi_I \left(\lambda_{s-1/2}^{-}; m', \beta' \right) \right\rangle = \frac{m}{\sqrt{s(2s+1)}} \delta_{m, m'} \delta_{\beta, \beta'} \quad (45)$$

$$\left\langle \xi_{+}^{(i)}(s, m, \beta) \middle| \Psi_{II} \left(\lambda_{s+1/2}^{+}; m', \beta' \right) \right\rangle = \frac{m}{\sqrt{(s+1)(2s+1)}} \delta_{m, m'} \delta_{\beta, \beta'}, \quad (46)$$

$$(47)$$

the other two being zero. We can now evaluate (42), using the fact that due to the unitary symmetry, every object has a block diagonal structure like (37). It is thus enough to calculate $\text{tr} \Pi_{\vec{A}B}^{(i)} \eta_{\vec{A}B}^{(i)}$ in the subspace of a fixed total spin s . Dropping the qubit indices for simplicity we obtain for the second term of (42):

$$\forall_{1 \leq i \leq N} \quad \text{tr} \Pi^{(i)}(s) \omega^{(i)}(s) = \text{tr} \rho(s)^{-1/2} \sigma^{(i)}(s) \rho(s)^{-1/2} \omega^{(i)}(s) \quad (48)$$

$$= \frac{1}{2^{2N-2}} \cdot \frac{1}{3} g^{[N-1]}(s) \frac{s(s+1)}{2s+1} \left[\left(\lambda_{s-1/2}^{-} \right)^{-1/2} - \left(\lambda_{s+1/2}^{+} \right)^{-1/2} \right]^2, \quad (49)$$

and last term in (43), which contains $|\Psi^+\rangle\langle\Psi^-|$. Vanishing term (43) and expression (49) are derived in Appendix B. Finally, putting all the steps together, we obtain the following entanglement fidelity:

$$F = \frac{1 + |\Gamma| \cos \theta}{2} F_{IH} + \frac{1 - |\Gamma| \cos \theta}{2} F_{corr}. \quad (50)$$

In the above expression F_{IH} is the Ishizaka-Hiroshima entanglement fidelity [1, 2]:

$$F_{IH} = \frac{1}{2^{N+3}} \sum_{k=0}^N \left(\frac{N-2k-1}{\sqrt{k+1}} + \frac{N-2k+1}{\sqrt{N-k+1}} \right)^2 \binom{N}{k}. \quad (51)$$

For the reader's convenience the term F_{IH} is calculated in Appendix D. The second term F_{corr} in (50) is the new entanglement fidelity correction term:

$$F_{corr} = \frac{1}{3} \cdot \frac{1}{2^N} \sum_{k=0}^N \binom{N}{k} [(N-2k)^2 - 1] \left(\frac{1}{\sqrt{k+1}} - \frac{1}{\sqrt{N-k+1}} \right)^2, \quad (52)$$

which behaves as $2/N + \mathcal{O}(1/N^2)$ for large N . This means that the correction term vanishes when $N \rightarrow \infty$ and the total entanglement fidelity (50) reads $F = \frac{1}{2}(1 + |\Gamma| \cos \theta)$ having maximum value 1 for $\theta = 0$ and $|\Gamma| = 1$ (no

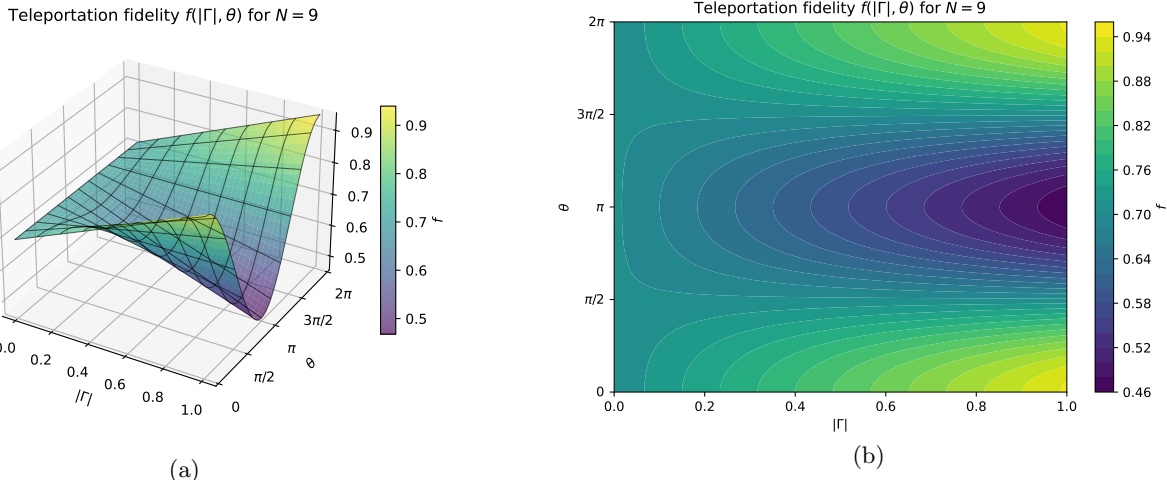


Figure 1 The average teleportation fidelity for $N = 9$, calculated using the entanglement fidelity Eq. (50), is plotted against $|\Gamma|$ and θ . The results are shown as (a) a three-dimensional surface plot and (b) a contour plot.

decoherence). Notice, that the function F_{corr} is not monotonic for small values of N . We observe monotonicity for larger values of N . The behaviour of F_{corr} , together with its derivation is presented in Appendix E.

A plot of the total resulting teleportation fidelity, $f = (2F + 1)/3$, as a function of $|\Gamma|$ and θ is presented in Fig. 1 for $N = 9$ (there is no qualitative change for different N). The no decoherence case corresponds on this plot to the corner $|\Gamma| = 1$ and $\theta = 0$. There is a pronounced minimum for $\theta = \pi$, which corresponds to the zeroing of the Ishizaka-Hiroshima term in (50), which is the dominating term. The maximum, of the other hand is obtained for $\theta = 0$, i.e. for a real decoherence factor Γ . This maximum can be obtained by a semi-adaptive procedure, where instead of using the original PGM, one rotates them by θ : $\Pi_i(\theta) = R^\dagger(\theta)_B \tilde{\Pi}_i^{\tilde{A}B} R(\theta)_B$. One can easily show, starting from (16), that this leads to the fidelity (50) with $\theta = 0$. Of course, this strategy assumes a partial knowledge about the noise, the phase of the decoherence factor θ , and the ability to use it for the POVM optimization. As we mentioned, for $\theta = 0$, the above strategy reduces to a special case of the Pauli noise channel, cf. (20), studied in [31]. Importantly, this qualitative picture persists in the asymptotic regime of large N . While the Ishizaka-Hiroshima contribution approaches unity as $N \rightarrow \infty$, the correction term F_{corr} vanishes as $\mathcal{O}(1/N)$. This is illustrated in Figure 2.

The fidelity obtained from (50) differs from that of [31] – it is always lower, at most by $\sim 10\%$ for $\Gamma = 0$, and becomes equal only for $\Gamma = 1$, where all three fidelities approach the Ishizaka-Hiroshima one. Detailed discussion on the Kim's approach is presented in Appendix F.

VI. PBT USING NOISE-ADAPTED MEASUREMENTS

The final, and the most complicated, scenario is that of discriminating measurements adapted to the noisy signal states (24). The natural choice here is of course again the PGM, but this time constructed from the noisy states $\eta_{\tilde{A}B}^{(i)}$. Following the general PGM recipe (29), one first has to find the average noisy ensemble state (we keep using un-normalized states):

$$\bar{\eta} = \sum_{i=1}^N \eta_{\tilde{A}B}^{(i)}. \quad (53)$$

Unlike for the noiseless average (36), there does not seem to be an obvious diagonalizing procedure for this state. First, the unitary symmetry of the noiseless case is lost whenever the decoherence is present, since the $A_i B$ part of each $\eta_{\tilde{A}B}^{(i)}$, given by \tilde{P}_{AB}^- , cf. (14), (24), does not have a definite symmetry under the product action of $SU(2)$, as we have explained below (29). Second, although each $\eta_{\tilde{A}B}^{(i)}$ can be easily diagonalized, cf. (25), they overlap on the qubit B making the diagonalization of the sum non-trivial. We thus have to resort to the numerics. We have employed in total three numerical methods, specifying to the case $\theta = 0$ expecting this is the best case scenario, cf. Fig. 1, and cross checking between the methods whenever possible:

(1) In the first method, the signal states $\eta_{\tilde{A}B}^{(i)}$ and the ensemble average (53) were constructed with a python program. The noisy PGM POVMs $\{\Pi_i\}$ were generated using the eigensolver of numpy library [49], where we first diagonalized

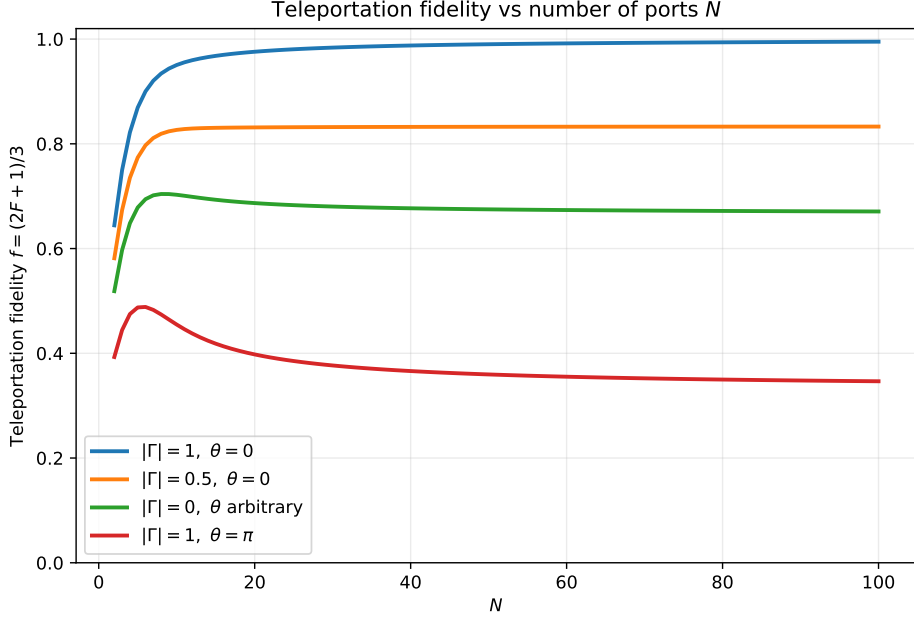


Figure 2 Teleportation fidelity $f = (2F + 1)/3$ as a function of N for four various choices of the noise parameters $(|\Gamma|, \theta)$. The blue line reproduces the noiseless case from the Hiroshima-Ishizaka protocol.

(53), discarded the zero eigenvalues, then constructed $\bar{\eta}^{-1/2}$ and from this the POVM's, checking numerically that the obtained operators were positive. The final POVM set included also the projector on the zero-eigenvalue subspace completeness. We finally computed (28) and from it the teleportation fidelity (3).

(2) In the second method, the starting point was the same, but the $\bar{\eta}^{-1/2}$ was computed differently, using the Taylor expansion:

$$\bar{\eta}^{-1/2} = \mathbb{1} - \frac{1}{2}(\bar{\eta} - \mathbb{1}) + \frac{3}{8}(\bar{\eta} - \mathbb{1})^2 - \frac{5}{16}(\bar{\eta} - \mathbb{1})^3 + \dots \quad (54)$$

and including the terms up to the order of 4000. The non-zero eigenspace gets perfectly inverted while the zero eigenspaces obviously diverge with the increased number of iterations. However, those terms disappear when the POVM's are constructed as the signal states $\eta^{(i)}$ turned out to be supported on subspaces orthogonal to the kernel of $\bar{\eta}$, which is rather a non-trivial observation, revealed by the numerics. The POVM's were again checked for the positivity, which was not an issue within the numerical precision due to the very high order of the expansion.

(3) The third method was a direct use of the Wolfram Mathematica program, which was feasible only for the simplest case of $N = 2$. We inserted the signal states by hand and then used the Mathematica eigensolver to diagonalize $\bar{\eta}$. From this, the POVM's were constructed and the teleportation fidelity computed.

All the three methods gave the same results within the numerical precision and whenever applicable. As a final cross-check, all the methods we also applied to the noiseless case of Section (V) and the confirmed the Eq. (50) for $\theta = 0$. The results are presented in Fig. 3(a) for $N = 2, 5, 9$ together with the noiseless curves and the Beigi-Koenig bound (35) for $N = 9$ for a comparison. Due to the exponential increase of the dimension, $d = 2^{N+1}$, $N = 9$ was the maximum available within a normal laptop capabilities but it turned out to be perfectly enough to reveal the behaviour of the considered strategies.

Quite surprisingly, the noise-adapted PGM performs worse than the noiseless PGM apart from $N = 2$. The noise-adapted strategy is better only in the region of strong decoherence, close to $\Gamma = 0$, but even that region is shrinking with increasing N , which is a bit of a surprise in its own right. The optimality of PGM for PBT [10] was shown only for the ideal case of uncorrupted Bell states, using the unitary symmetry. There are no general optimality results for PGM, apart from, so called, geometrically uniform ensembles, where the ensemble states are generated from a reference state by application of unitaries from a given symmetry group. In this case, the PGM is known to be optimal for pure state ensembles and for mixed states with some additional condition (Theorem 3 of [50]; see also [51]). It is thus not that surprising that PGM ceases to be optimal in the presence of decoherence, what is however surprising is that it is beaten by the noiseless PGM, which is completely agnostic to the changes in the ensemble introduced by the decoherence.

As a final remark, there is of course a case when the optimal, noisy measurement is known: For $N = 2$ there

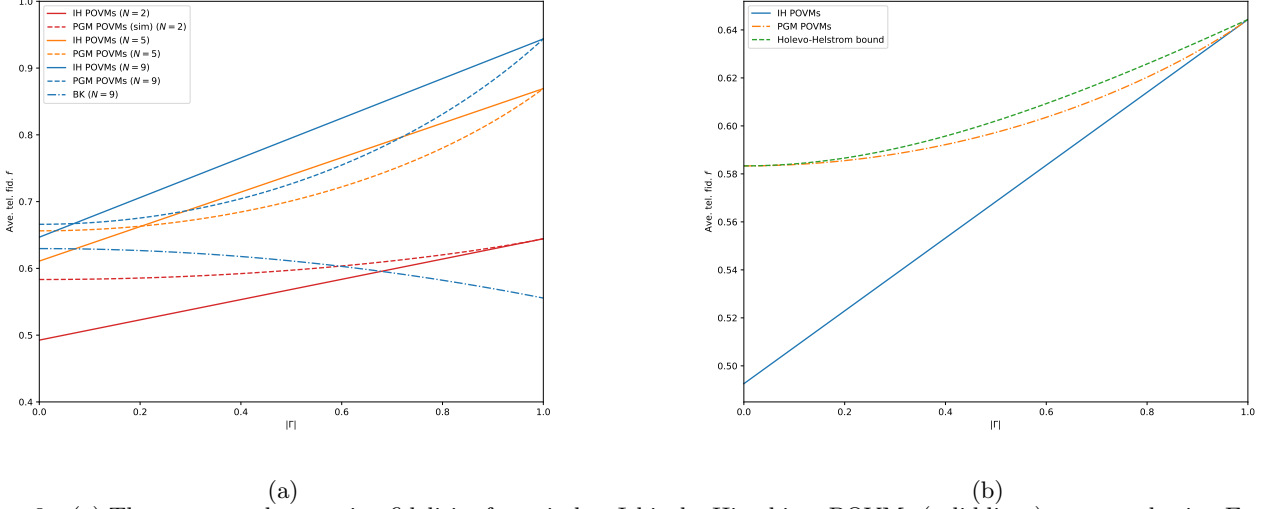


Figure 3 (a) The average teleportation fidelities for noiseless Ishizaka-Hiroshima POVMs (solid lines) computed using Eq. (50) and the average teleportation fidelities for PGM (dashed lines) computed using eigensolver python program are plotted for $N = 2, 5, 9$. The Beigi-König bound for $N = 9$ is plotted with blue dashed-dotted line. (b) Average teleportation fidelities for noiseless POVMs (blue solid), PGM (orange dashed-dotted) and the maximum fidelity as per Helstrom bound (green dashed) are plotted for $N = 2$.

is the famous Helstrom optimality bound [52], given in the terms of the trace distance between the states $P_{\text{succ}} \leq 1/2 + (1/4)\|\eta^{(1)} - \eta^{(2)}\|_1$. A direct calculation shows that (see Appendix C):

$$\|\eta^{(1)} - \eta^{(2)}\|_1 = \sqrt{1 + 2|\Gamma|^2}, \quad (55)$$

and therefore the entanglement fidelity is upper-bounded for $N = 2$ by:

$$F \leq \frac{1}{4} \left(1 + \frac{\sqrt{1 + 2|\Gamma|^2}}{2} \right). \quad (56)$$

The plot of this bound together with the PGM fidelity for both noiseless and noise-adapted scenarios is presented in Fig. 3(b). There is a substantial gain w.r.t. the noiseless measurement and only a slight one w.r.t. the noise-adapted one.

VII. CASE STUDY: SPIN-BOSON MODEL

In this section we provide a concrete realization of the pure-dephasing model used throughout the paper. We will use the well known spin boson model, which has been one of the standard models describing decoherence effects of qubits. We will assume the self-Hamiltonian of the qubits is suppressed, which is motivated by the fact that one would like to produce Bell states for each pair and keep the qubits in those states. This leads to the pure-dephasing evolution, analysed above, where all the information about the interaction with the environment is encoded in the complex decoherence parameter

$$\Gamma(t, r) = |\Gamma(t, r)|e^{i\theta(t, r)}. \quad (57)$$

We assume position-dependent coupling to the bath, depending explicitly on the spatial separation r between the qubits forming each Bell pair. This mimics the interaction e.g. with the electromagnetic field. We consider a generalized Ohmic spectral density with an exponential cutoff,

$$J(\omega) = \frac{\omega^s}{\Lambda^{s-1}} e^{-\omega/\Lambda}, \quad (58)$$

where Λ is a high-frequency cutoff and s is the Ohmicity exponent. Introducing dimensionless variables

$$\tau = t\Lambda, \quad \vartheta = \frac{T}{\Lambda}, \quad (59)$$

it is convenient to parametrize the separation dependence by the dimensionless distance parameter

$$\ell = \frac{r\Lambda}{c}. \quad (60)$$

In terms of these variables, the decoherence factor takes the form

$$\Gamma(\tau, \ell) = \exp[-\chi(\tau, \ell) + i\theta(\tau, \ell)], \quad (61)$$

where the explicit expressions for $\chi(\tau, \ell)$ and $\theta(\tau, \ell)$ are derived in Appendix G as,

$$\chi(\tau, \ell) = 2 \int_0^\infty d\tilde{\omega} \tilde{\omega}^{s-2} e^{-\tilde{\omega}} (1 - \cos(\tilde{\omega}\tau)) \coth\left(\frac{\tilde{\omega}}{2\vartheta}\right) [1 - \cos(\tilde{\omega}\ell)], \quad (62)$$

$$\theta(\tau, \ell) = \frac{1}{2} \int_0^\infty d\tilde{\omega} \tilde{\omega}^{s-2} e^{-\tilde{\omega}} (1 - \cos(\tilde{\omega}\tau)) \sin(\tilde{\omega}\ell). \quad (63)$$

The integrals can be calculated explicitly for $s > 1$, see e.g. [45]. More details are recalled in Appendix G. We also recall that independently of the microscopic structure of the bath, the reduced state of each Bell pair after tracing out the environment can always be written in the form

$$\tilde{P}_{AB}^-(t, r) = (\mathbb{1} \otimes \mathcal{E}_{\Gamma(t, r)})(P_{AB}^-), \quad (64)$$

so that all results derived in Secs. V and VI remain valid after the substitution $\Gamma \rightarrow \Gamma(t, r)$.

We first consider noiseless Ishizaka–Hiroshima measurements as they can be analyzed analytically. The entanglement fidelity of the teleportation channel then reads

$$F(\tau, \ell) = \frac{1 + |\Gamma(\tau, \ell)| \cos \theta(\tau, \ell)}{2} F_{\text{IH}} + \frac{1 - |\Gamma(\tau, \ell)| \cos \theta(\tau, \ell)}{2} F_{\text{corr}}, \quad (65)$$

and the corresponding teleportation fidelity is

$$f(\tau, \ell) = \frac{2F(\tau, \ell) + 1}{3}. \quad (66)$$

We plot it as a function of the dimensionless time $\tau = t\Lambda$, in Fig. 4a,b solid lines. Two representative values of the temperature, $T/\Lambda = 0.1$ and $T/\Lambda = 0.9$, are chosen to contrast low- and high-temperature environments relative to the cutoff. Increasing T/Λ enhances thermal decoherence, leading to a faster suppression of the fidelity at long times, while the short-time behaviour is only weakly affected.

The case for noise-adapted measurements is studied numerically by taking Γ as a function of τ . Unlike Section VI, we consider the complex value of decoherence factor with $\chi(\tau, \ell)$ and $\theta(\tau, \ell)$ given in (63). The inverse square root of the ensemble state is computed using the eigensolver method. The results are summarized in Figure 4, dashed lines. As we have predicted before, surprisingly noise-adapted measurements perform worse than the noiseless ones, even with a large temperature difference.

We can see characteristic dips in the teleportation fidelity, so that it is not monotonically decreasing with time even for $s = 2$. These dips are associated with a finite time-of-flight of the field quanta between the qubits' positions. In the simulations shown in Fig. 4 the spatial separation is fixed to $\ell = \Lambda r/c = 3$. That distance enters the decoherence factor through the oscillatory terms in (62)–(63). The dips are centered exactly at $\tau \simeq 3$, corresponding to the time scale at which the distance-dependent phase $\theta(\tau, \ell)$ produces destructive interference in the coherence factor $\Gamma(\tau, \ell)$ through the $\cos \theta(\tau, \ell)$ term. Memory effects are reflected in the non-exponential short-time behaviour of $F(\tau, \ell)$, whereas the long-time dynamics is controlled by the saturation of $\chi(\tau, \ell)$, explaining why increasing temperature primarily lowers the asymptotic fidelity plateau observed in Fig. 4.

VIII. DISCUSSION AND CONCLUSION

In this work we have analysed deterministic PBT in the presence of pure-dephasing decoherence affecting both the entangled resource state and the measurement process. Our primary objective was to understand how proposed noise models modify the performance of the PBT protocol and to identify regimes in which analytical control can still be maintained. To this end, we focused on a setting in which each Bell pair forming the resource state interacts with its own identical local environment, corresponding to independently distributed entangled links. This choice captures still an experimentally relevant scenario while preserving sufficient symmetry to allow for explicit analysis.

We considered two complementary noisy scenarios:

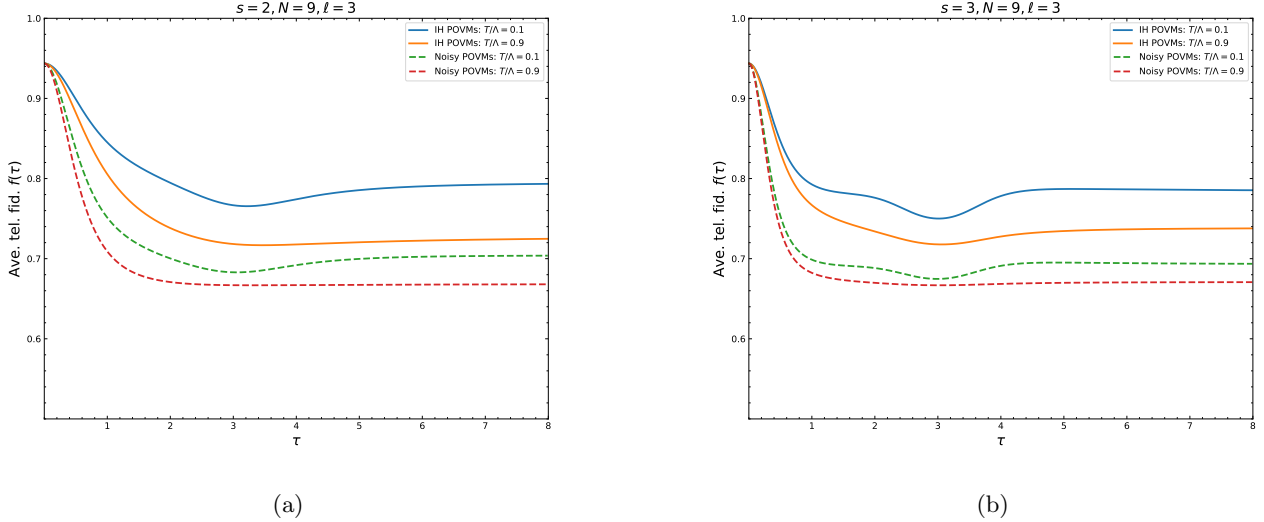


Figure 4 Average teleportation fidelity $f(\tau)$ for $N = 9$ as a function of the dimensionless time $\tau = t\Lambda$ for a generalized Ohmic bath with Ohmicity $s = 2$ ($s = 3$) and transit time $\ell = \Lambda\bar{t} = 3$. Solid lines – noiseless measurements; dashed lines – noise-adapted measurements. Each curve corresponds to a fixed temperature ratio $T/\Lambda = 0.1$ or $T/\Lambda = 0.9$.

- Decoherence acts only on the resource state while Alice’s measurement is assumed to be ideal. In this case, we derived a lower bound on the teleportation fidelity and derived a closed-form expression for the fidelity valid for arbitrary numbers of ports. This enabled us to analyse the asymptotic behaviour of the protocol and to show that, while decoherence expectedly lowers the fidelity compared to the Ishizaka–Hiroshima result, the correction term vanishes when the resource state grows, leaving the overall qualitative behaviour unchanged in the asymptotic regime.
- In the second scenario, we addressed the problem of noisy measurements and introduced noise-adapted POVMs tailored to the given decoherence model, which in this case means using the pretty good measurements, constructed from the noisy ensemble. While a fully analytical treatment appears out of reach for a general N , we demonstrated that a semi-analytical approach combined with numerical optimisation yields performance estimates. Moreover, for the special case $N = 2$, we derived an explicit analytical lower bound on the entanglement fidelity based on the Helstrom optimality bound, providing a useful benchmark for assessing the performance of noise-adapted measurements. Quite surprisingly, we find that noise-adapted measurements perform worse for finite N than the ideal, noise-agnostic ones.

Further, to connect with microscopic physical models, we embedded the protocol into a spin–boson framework and parametrised the environment in terms of dimensionless quantities controlling bath memory, temperature, cut-off, and the interaction time. By analysing representative super-Ohmic regimes $s = 2$ and $s = 3$ and temperatures, we demonstrated that the temperature has predictably a strong effect on the fidelity while the Ohmicity in this case has only a moderate influence, unlike for a single spin models, where the transition from $s = 2$ to $s = 3$ corresponds to the change from Markovian to non-Markovian regimes. We thereby illustrated the sensitivity of the PBT protocol to microscopic noise properties beyond depolarising models.

Several directions for future work naturally emerge from our analysis. An important extension would be to consider common or correlated environments acting on multiple Bell pairs, which may give rise to collective decoherence effects not captured by the present model. Another open problem is the systematic optimisation of noisy measurements for general N , potentially exploiting additional symmetries, like residual covariance with respect to the group $U(1)_Z \times S_N$, or approximate covariance properties to reduce computational complexity. From a physical perspective, it would also be interesting to investigate other classes of environments, as well as to explore experimentally motivated noise-mitigation strategies within the PBT framework, e.g. similar to the so-called purifying teleportation [44]. We believe that the methods developed here provide a solid starting point for addressing these questions and for future work.

ACKNOWLEDGMENTS

MS is supported by the National Science Centre, Poland, Grant Sonata Bis 14 no. 2024/54/E/ST2/00316. RSB and JKK acknowledge the support of National Science Centre (NCN) through the QuantEra project Qucabose 2023/05/Y/ST2/00139.

Appendix A: Fidelity between $\eta^{(i)}$ and $\eta^{(j)}$

The state fidelity between two signal states $\eta^{(i)}$ and $\eta^{(j)}$ is defined as

$$F(\eta^{(i)}, \eta^{(j)}) = \text{tr} \sqrt{\sqrt{\eta^{(i)}} \eta^{(j)} \sqrt{\eta^{(i)}}}. \quad (\text{A1})$$

Using (24), (26), and (27) we immediately find that:

$$\sqrt{\eta^{(i)}} = R(\theta)_B \left[\sqrt{\frac{1+|\Gamma|}{2}} |\Psi^-\rangle\langle\Psi^-| + \sqrt{\frac{1-|\Gamma|}{2}} |\Psi^+\rangle\langle\Psi^+| \right] R(\theta)_B^\dagger \otimes \frac{\mathbb{1}_{\bar{A}_i}}{\sqrt{2^{N-1}}} \quad (\text{A2})$$

Lengthy but straightforward calculations show that:

$$\sqrt{\eta^{(i)}} \eta^{(j)} \sqrt{\eta^{(i)}} = R(\theta) \nu_{A_i A_j B} R(\theta)^\dagger \otimes \frac{\mathbb{1}_{\bar{A}_{ij}}}{2^{2(N-2)}}, \quad (\text{A3})$$

where

$$\nu_{A_i A_j B} \equiv \frac{1}{32} [(1 + \sqrt{1 - |\Gamma|^2})(|001\rangle\langle 001| + |110\rangle\langle 110|) + (1 - \sqrt{1 - |\Gamma|^2})(|011\rangle\langle 011| + |100\rangle\langle 100|) \quad (\text{A4})$$

$$- |\Gamma| (|001\rangle\langle 100| + |011\rangle\langle 110| + |100\rangle\langle 001| + |110\rangle\langle 011|)]. \quad (\text{A5})$$

This is a 4×4 matrix, which has a simple block diagonal form with the following matrix on the diagonal:

$$\frac{1}{32} \begin{pmatrix} 1 + \sqrt{1 + |\Gamma|^2} & -|\Gamma| \\ -|\Gamma| & 1 - \sqrt{1 + |\Gamma|^2} \end{pmatrix}, \quad (\text{A6})$$

which has eigenvalues 0 and $2/32 = 1/16$. We thus obtain:

$$\text{tr} \sqrt{\sqrt{\eta^{(i)}} \eta^{(j)} \sqrt{\eta^{(i)}}} = \text{tr} \sqrt{R(\theta)_B \nu_{A_i A_j B} R(\theta)_B^\dagger} = \text{tr} \sqrt{\nu_{A_i A_j B}} = \frac{1}{4} + \frac{1}{4} \quad (\text{A7})$$

and therefore:

$$F(\eta^{(i)}, \eta^{(j)}) = \frac{1}{2}, \quad (\text{A8})$$

which is constant, independent of both N and Γ .

Appendix B: Calculations the noiselss measurements

Eigenstates of ρ , two families from the spin-1/2 addition to $N-2$ spins, one family corresponds to $j+1/2$, second to $j-1/2$

$$\begin{aligned} |\Psi_I(\lambda_j^\pm; m, \beta)\rangle &= \left| \Phi^{[N-1]}(j + \frac{1}{2}, m + 1, \beta) \right\rangle_{\bar{A}_i} |0\rangle_{A_i} |0\rangle_B \left\langle j, m + \frac{1}{2}, \frac{1}{2}, -\frac{1}{2} \middle| j \pm \frac{1}{2}, m \right\rangle \left\langle j + \frac{1}{2}, m + 1, \frac{1}{2}, -\frac{1}{2} \middle| j, m + \frac{1}{2} \right\rangle \\ &+ \left| \Phi^{[N-1]}(j + \frac{1}{2}, m, \beta) \right\rangle_{\bar{A}_i} |1\rangle_{A_i} |0\rangle_B \left\langle j, m + \frac{1}{2}, \frac{1}{2}, -\frac{1}{2} \middle| j \pm \frac{1}{2}, m \right\rangle \left\langle j + \frac{1}{2}, m, \frac{1}{2}, \frac{1}{2} \middle| j, m + \frac{1}{2} \right\rangle \\ &+ \left| \Phi^{[N-1]}(j + \frac{1}{2}, m, \beta) \right\rangle_{\bar{A}_i} |0\rangle_{A_i} |1\rangle_B \left\langle j, m - \frac{1}{2}, \frac{1}{2}, \frac{1}{2} \middle| j \pm \frac{1}{2}, m \right\rangle \left\langle j + \frac{1}{2}, m, \frac{1}{2}, -\frac{1}{2} \middle| j, m - \frac{1}{2} \right\rangle \\ &+ \left| \Phi^{[N-1]}(j + \frac{1}{2}, m - 1, \beta) \right\rangle_{\bar{A}_i} |1\rangle_{A_i} |1\rangle_B \left\langle j, m - \frac{1}{2}, \frac{1}{2}, \frac{1}{2} \middle| j \pm \frac{1}{2}, m \right\rangle \left\langle j + \frac{1}{2}, m - 1, \frac{1}{2}, \frac{1}{2} \middle| j, m - \frac{1}{2} \right\rangle \end{aligned} \quad (\text{B1})$$

and

$$\begin{aligned}
|\Psi_{\text{II}}(\lambda_j^{\mp}; m, \beta)\rangle &= \left| \Phi^{[N-1]}(j - \frac{1}{2}, m+1, \beta) \right\rangle_{\bar{A}_i} |0\rangle_{A_i} |0\rangle_B \left\langle j, m + \frac{1}{2}, \frac{1}{2}, -\frac{1}{2} \middle| j \pm \frac{1}{2}, m \right\rangle \left\langle j - \frac{1}{2}, m+1, \frac{1}{2}, -\frac{1}{2} \middle| j, m + \frac{1}{2} \right\rangle \\
&+ \left| \Phi^{[N-1]}(j - \frac{1}{2}, m, \beta) \right\rangle_{\bar{A}_i} |1\rangle_{A_i} |0\rangle_B \left\langle j, m + \frac{1}{2}, \frac{1}{2}, -\frac{1}{2} \middle| j \pm \frac{1}{2}, m \right\rangle \left\langle j - \frac{1}{2}, m, \frac{1}{2}, \frac{1}{2} \middle| j, m + \frac{1}{2} \right\rangle \\
&+ \left| \Phi^{[N-1]}(j - \frac{1}{2}, m, \beta) \right\rangle_{\bar{A}_i} |0\rangle_{A_i} |1\rangle_B \left\langle j, m - \frac{1}{2}, \frac{1}{2}, \frac{1}{2} \middle| j \pm \frac{1}{2}, m \right\rangle \left\langle j - \frac{1}{2}, m, \frac{1}{2}, -\frac{1}{2} \middle| j, m - \frac{1}{2} \right\rangle \\
&+ \left| \Phi^{[N-1]}(j - \frac{1}{2}, m-1, \beta) \right\rangle_{\bar{A}_i} |1\rangle_{A_i} |1\rangle_B \left\langle j, m - \frac{1}{2}, \frac{1}{2}, \frac{1}{2} \middle| j \pm \frac{1}{2}, m \right\rangle \left\langle j - \frac{1}{2}, m-1, \frac{1}{2}, \frac{1}{2} \middle| j, m - \frac{1}{2} \right\rangle
\end{aligned} \tag{B2}$$

$$\sigma^{(i)} = \sum_{s=s_{\min}}^{(N-1)/2} \sigma^{(i)}(s), \tag{B3}$$

with

$$\sigma^{(i)}(s) = \frac{1}{2^{N-1}} \sum_{m=-s}^s \sum_{\beta} \left| \xi_-^{(i)}(s, m, \beta) \right\rangle \left\langle \xi_-^{(i)}(s, m, \beta) \right| . \tag{B4}$$

and similarly:

$$\omega^{(i)} = \sum_{s=s_{\min}}^{(N-1)/2} \omega^{(i)}(s), \tag{B5}$$

$$\omega^{(i)}(s) = \frac{1}{2^{N-1}} \sum_{m=-s}^s \sum_{\beta} \left| \xi_+^{(i)}(s, m, \beta) \right\rangle \left\langle \xi_+^{(i)}(s, m, \beta) \right| . \tag{B6}$$

Borrowing from Ishizaka *et. al.*, For a comparison, in the IH calculation:

$$\text{tr} \Pi^{(i)}(s) \sigma^{(i)}(s) = g^{[N-1]}(s) \frac{1}{2s+1} \left[s \left(\lambda_{s-1/2}^- \right)^{-1/2} + (s+1) \left(\lambda_{s+1/2}^+ \right)^{-1/2} \right]^2 \tag{B7}$$

$$\text{tr} \Pi^{(i)}(s) \omega^{(i)}(s) = \text{tr} \rho(s)^{-1/2} \sigma^{(i)}(s) \rho(s)^{-1/2} \omega^{(i)}(s) \tag{B8}$$

$$= \sum_{m, m'=-s}^s \sum_{\beta, \beta'} \left| \left\langle \xi_+^{(i)}(s, m', \beta') \right| \rho(s)^{-1/2} \left| \xi_-^{(i)}(s, m, \beta) \right\rangle \right|^2 \tag{B9}$$

$$= \sum_{\beta} \sum_{m=-s}^s \frac{m^2}{(2s+1)^2} \left[\left(\lambda_{s-1/2}^- \right)^{-1/2} - \left(\lambda_{s+1/2}^+ \right)^{-1/2} \right]^2 \tag{B10}$$

$$= \sum_{\beta} \frac{s(s+1)(2s+1)}{3} \frac{1}{(2s+1)^2} \left[\left(\lambda_{s-1/2}^- \right)^{-1/2} - \left(\lambda_{s+1/2}^+ \right)^{-1/2} \right]^2 \tag{B11}$$

$$= \frac{1}{3} g^{[N-1]}(s) \frac{s(s+1)}{2s+1} \left[\left(\lambda_{s-1/2}^- \right)^{-1/2} - \left(\lambda_{s+1/2}^+ \right)^{-1/2} \right]^2 . \tag{B12}$$

Here, we have used $\sum_{m=-s}^s m^2 = \frac{1}{3}s(s+1)(2s+1)$ and $\sum_{\beta} = g^{[N-1]}(s)$ is the intrinsic degeneracy for $|\Psi_{\text{I}}(\lambda_{s-1/2}^-; m, \beta)\rangle$ and $|\Psi_{\text{II}}(\lambda_{s+1/2}^+; m, \beta)\rangle$. Further simplification of the above term is presented in Appendix E.

Now, we show vanishing of expression (43). We have the following:

$$\text{tr} \Pi_{AB}^{(i)} \left[(|\Psi^+\rangle\langle\Psi^-| - |\Psi^-\rangle\langle\Psi^+|)_{A_i B} \otimes \frac{\mathbf{1}_{\bar{A}_i}}{2^{N-1}} \right] = \quad (\text{B13})$$

$$= \frac{1}{2^{N-1}} \sum_s \sum_{m,\beta} \left\{ \left\langle \xi_-^{(i)}(s, m, \beta) \right| \Pi^{(i)}(s) \left| \xi_+^{(i)}(s, m, \beta) \right\rangle - c.c. \right\} \quad (\text{B14})$$

$$= \frac{1}{2^{N-1}} \sum_s \sum_{m, m', \beta, \beta'} \left\{ \left\langle \xi_-^{(i)}(s, m, \beta) \right| \rho(s)^{-1/2} \left| \xi_-^{(i)}(s, m', \beta') \right\rangle \left\langle \xi_-^{(i)}(s, m', \beta') \right| \rho(s)^{-1/2} \left| \xi_+^{(i)}(s, m', \beta') \right\rangle - c.c. \right\} \quad (\text{B15})$$

$$= \frac{1}{2^{N-1}} \sum_s \sum_m g^{[N-1]}(s) \left\{ c_{IH}(s) \frac{m}{2s+1} \left[\left(\lambda_{s-1/2}^- \right)^{-1/2} - \left(\lambda_{s+1/2}^+ \right)^{-1/2} \right] - c.c. \right\} = 0. \quad (\text{B16})$$

Where, $c_{IH}(s) = \left\langle \xi_-^{(i)}(s, m, \beta) \right| \rho(s)^{-1/2} \left| \xi_-^{(i)}(s, m', \beta') \right\rangle$. Since $\sum_m m = 0$, actually not only all the overlaps above are real and hence their imaginary part is zero, but each term $\sum_m \left\langle \xi_-^{(i)}(s, m, \beta) \right| \Pi^{(i)}(s) \left| \xi_+^{(i)}(s, m, \beta) \right\rangle$ vanishes on its own.

Appendix C: Explicit derivations from the Helstrom bound

The goal of this Appendix is to prove expression (56) from the main text, which reads:

$$F \leq \frac{1}{4} \left(1 + \frac{\sqrt{1+2|\Gamma|^2}}{2} \right). \quad (\text{C1})$$

For $N = 2$, the noisy states entering the binary discrimination problem are

$$\eta_{A_1 A_2 B}^{(i)} = R_B(\theta) \left[\frac{1+|\Gamma|}{2} \sigma_{A_1 A_2 B}^{(i)} + \frac{1-|\Gamma|}{2} \omega_{A_1 A_2 B}^{(i)} \right] R_B(\theta)^\dagger, \quad i = 1, 2, \quad (\text{C2})$$

with

$$\sigma_{A_1 A_2 B}^{(1)} = \frac{1}{2} |\Psi^-\rangle\langle\Psi^-|_{A_1 B} \otimes \mathbf{1}_{A_2}, \quad \omega_{A_1 A_2 B}^{(1)} = \frac{1}{2} |\Psi^+\rangle\langle\Psi^+|_{A_1 B} \otimes \mathbf{1}_{A_2}, \quad (\text{C3})$$

$$\sigma_{A_1 A_2 B}^{(2)} = \frac{1}{2} \mathbf{1}_{A_1} \otimes |\Psi^-\rangle\langle\Psi^-|_{A_2 B}, \quad \omega_{A_1 A_2 B}^{(2)} = \frac{1}{2} \mathbf{1}_{A_1} \otimes |\Psi^+\rangle\langle\Psi^+|_{A_2 B}. \quad (\text{C4})$$

We define the difference operator

$$\Delta := \eta^{(1)} - \eta^{(2)}. \quad (\text{C5})$$

Since both $\eta^{(1)}$ and $\eta^{(2)}$ are conjugated by the same unitary $R_B(\theta)$, the trace norm is invariant under this transformation and

$$\|\Delta\|_1 = \|\Delta_0\|_1, \quad \Delta_0 := \frac{1+|\Gamma|}{2} (\sigma^{(1)} - \sigma^{(2)}) + \frac{1-|\Gamma|}{2} (\omega^{(1)} - \omega^{(2)}). \quad (\text{C6})$$

Hence, the phase θ does not affect the Helstrom bound, and only $|\Gamma|$ enters.

Notice that in this case the operators $\sigma^{(i)}$ and $\omega^{(i)}$ differ only by which port is paired with the system B . It means that Δ_0 is antisymmetric under the exchange of the two ports $A_1 \leftrightarrow A_2$. It follows that Δ_0 vanishes on the symmetric subspace of $A_1 A_2$ and acts non-trivially only on a two-dimensional sector. In particular, Δ_0 is Hermitian, traceless, and has rank at most 2. In the B respecting these symmetries

$$B = \left\{ |00\rangle|0\rangle, |00\rangle|1\rangle, |\psi_+\rangle|0\rangle, |\psi_+\rangle|1\rangle, |11\rangle|0\rangle, |11\rangle|1\rangle; |\psi_-\rangle|0\rangle, |\psi_-\rangle|1\rangle \right\}, \quad (\text{C7})$$

the term Δ_0 has the following explicit form:

$$\Delta_0 = \begin{pmatrix} 0_{6 \times 6} & M \\ M^\dagger & 0_{2 \times 2} \end{pmatrix}, \quad M = \begin{pmatrix} 0 & 0 \\ \sqrt{2}|\Gamma|/4 & 0 \\ -1/4 & 0 \\ 0 & 1/4 \\ 0 & -\sqrt{2}|\Gamma|/4 \\ 0 & 0 \end{pmatrix}. \quad (\text{C8})$$

Notice that the first 6 vectors of the basis B in (C7) span the symmetric space $\text{Sym}(A_1 A_2) \otimes B$, while the last 2 span the antisymmetric sector $\text{Asym}(A_1 A_2) \otimes B$.

A direct diagonalization of Δ_0 on this sector yields the nonzero eigenvalues

$$\lambda_{\pm} = \pm \frac{1}{2} \sqrt{1 + 2|\Gamma|^2}, \quad (\text{C9})$$

while all remaining eigenvalues are zero. Since Δ is Hermitian, its trace norm equals the sum of absolute values of its eigenvalues, and thus

$$\|\eta^{(1)} - \eta^{(2)}\|_1 = |\lambda_+| + |\lambda_-| = \sqrt{1 + 2|\Gamma|^2}, \quad (\text{C10})$$

which proves Eq. (C1).

Appendix D: Derivation of expression (29) from [2]

For the Reader's convenience, we derive here expression (51) for the entanglement fidelity F_{IH} for the noiseless deterministic PBT reported for the first time in [1, 2]. Starting from the expression for the entanglement fidelity under the square-root measurement (SRM), see the second line of equation (29) in [2], we have:

$$F_{IH} = \frac{N}{2^{2N}} \sum_{s=s_{\min}}^{(N-1)/2} (2s+1) g^{[N-1]}(s) [c(s, 2)]^2, \quad (\text{D1})$$

where

$$c(s, y) = \frac{s}{2s+1} (\lambda_{s-1/2}^-)^{-1/y} + \frac{s+1}{2s+1} (\lambda_{s+1/2}^+)^{-1/y}, \quad (\text{D2})$$

and the eigenvalues of ρ are

$$\lambda_{s-1/2}^- = \frac{N-2s+1}{2^{N+1}}, \quad \lambda_{s+1/2}^+ = \frac{N+2s+3}{2^{N+1}}. \quad (\text{D3})$$

a. *Step 1: Substitute eigenvalues.* For $y=2$, Eq. (D2) gives

$$c(s, 2) = \frac{s}{2s+1} \sqrt{\frac{2^{N+1}}{N-2s+1}} + \frac{s+1}{2s+1} \sqrt{\frac{2^{N+1}}{N+2s+3}}. \quad (\text{D4})$$

b. *Step 2: Change of variables.* Let $k = \frac{N-1}{2} - s$, so that

$$N-2s+1 = 2(k+1), \quad N+2s+3 = 2(N-k+1).$$

Then Eq. (D4) becomes

$$c(s, 2) = \frac{2^{(N-1)/2}}{2s+1} \left(\frac{s}{\sqrt{k+1}} + \frac{s+1}{\sqrt{N-k+1}} \right). \quad (\text{D5})$$

c. *Step 3: Insert into (D1).* Squaring and substituting into (D1) yields

$$F_{IH} = \frac{N}{2^{N+1}} \sum_{s=s_{\min}}^{(N-1)/2} \frac{g^{[N-1]}(s)}{2s+1} \left(\frac{s}{\sqrt{k+1}} + \frac{s+1}{\sqrt{N-k+1}} \right)^2. \quad (\text{D6})$$

d. *Step 4: Express multiplicity as a binomial coefficient.* From Eq. (9) of the paper (with $N \rightarrow N-1$),

$$g^{[N-1]}(s) = \frac{(2s+1)(N-1)!}{\left(\frac{N-1}{2} - s\right)! \left(\frac{N+1}{2} + s\right)!} = \frac{(2s+1)(N-1)!}{k!(N-k)!}. \quad (\text{D7})$$

Hence

$$\frac{g^{[N-1]}(s)}{2s+1} = \frac{1}{N} \binom{N}{k}.$$

Substituting into (D6) cancels the prefactor N :

$$F_{IH} = \frac{1}{2^{N+1}} \sum_{k=0}^N \binom{N}{k} \left(\frac{s}{\sqrt{k+1}} + \frac{s+1}{\sqrt{N-k+1}} \right)^2. \quad (\text{D8})$$

e. *Step 5: Express s in terms of k .* Since $s = \frac{N-1}{2} - k$, we have

$$\frac{s}{\sqrt{k+1}} = \frac{N-2k-1}{2\sqrt{k+1}}, \quad \frac{s+1}{\sqrt{N-k+1}} = \frac{N-2k+1}{2\sqrt{N-k+1}}.$$

Plugging this in yields the final compact form:

$$\boxed{F_{IH} = \frac{1}{2^{N+3}} \sum_{k=0}^N \left(\frac{N-2k-1}{\sqrt{k+1}} + \frac{N-2k+1}{\sqrt{N-k+1}} \right)^2 \binom{N}{k}}. \quad (\text{D9})$$

Appendix E: Calculating closed-form expression for F_{corr}

We start from expression (48). The correction term F_{corr} can be calculated as

$$F_{\text{corr}} = \sum_{i=1}^N \sum_{s=s_{\min}}^{(N-1)/2} \text{tr} \Pi^{(i)}(s) \omega^{(i)}(s) = N \sum_{s=s_{\min}}^{(N-1)/2} \text{tr} \Pi^{(N)}(s) \omega^{(N)}(s). \quad (\text{E1})$$

Plugging the explicit expression for $\text{tr} \Pi^{(N)}(s) \omega^{(N)}(s)$ from (49), we have

$$F_{\text{corr}} = \frac{N}{2^{2N-2}} \sum_{s=s_{\min}}^{(N-1)/2} \frac{1}{3} g^{[N-1]}(s) \frac{s(s+1)}{2s+1} \left[\left(\lambda_{s-\frac{1}{2}}^- \right)^{-1/2} - \left(\lambda_{s+\frac{1}{2}}^+ \right)^{-1/2} \right]^2, \quad (\text{E2})$$

with eigenvalues of ρ

$$\lambda_{s-1/2}^- = \frac{N-2s+1}{2^{N+1}}, \quad \lambda_{s+1/2}^+ = \frac{N+2s+3}{2^{N+1}}, \quad (\text{E3})$$

and multiplicity (for $N \rightarrow N-1$)

$$g^{[N-1]}(s) = \frac{(2s+1)(N-1)!}{\left(\frac{N-1}{2} - s\right)! \left(\frac{N+1}{2} + s\right)!}. \quad (\text{E4})$$

a. *Step 1: Substitute the eigenvalues.* From (E3),

$$\left(\lambda_{s-1/2}^- \right)^{-1/2} - \left(\lambda_{s+1/2}^+ \right)^{-1/2} = 2^{\frac{N+1}{2}} \left(\frac{1}{\sqrt{N-2s+1}} - \frac{1}{\sqrt{N+2s+3}} \right).$$

b. *Step 2: Change of variables.* Let

$$k = \frac{N-1}{2} - s \iff s = \frac{N-1}{2} - k, \quad k = 0, 1, \dots, N. \quad (\text{E5})$$

Then

$$N-2s+1 = 2(k+1), \quad N+2s+3 = 2(N-k+1), \quad 2s+1 = N-2k,$$

and

$$s(s+1) = \frac{(2s+1)^2 - 1}{4} = \frac{(N-2k)^2 - 1}{4}. \quad (\text{E6})$$

Hence

$$\left[\left(\lambda_{s-\frac{1}{2}}^- \right)^{-1/2} - \left(\lambda_{s+\frac{1}{2}}^+ \right)^{-1/2} \right]^2 = 2^N \left(\frac{1}{\sqrt{k+1}} - \frac{1}{\sqrt{N-k+1}} \right)^2. \quad (\text{E7})$$

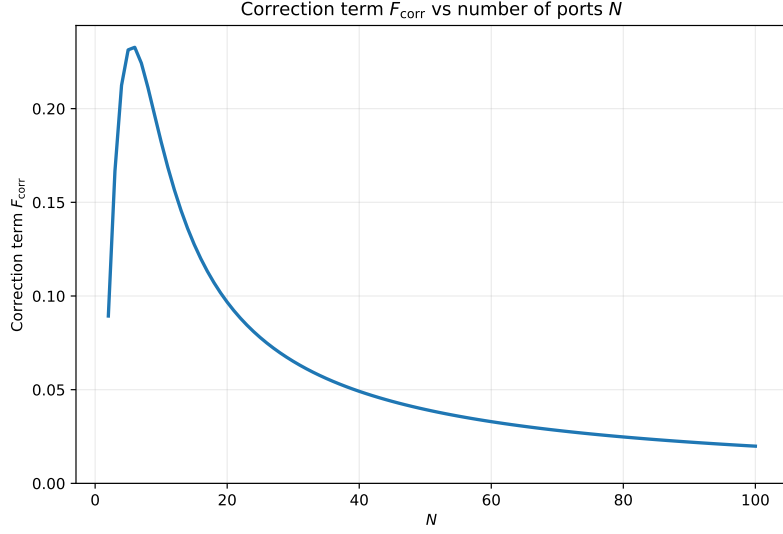


Figure 5 The correction term F_{corr} from expression (E10). We see non-monotonicity behaviour for small value of N . The function F_{corr} achieves maximum value $F_{\text{corr}} \approx 0.2327$ for $N = 6$. For $N > 6$ the correction term vanishes monotonically, achieving 0 for $N \rightarrow \infty$.

c. *Step 3: Convert multiplicities to binomials.* Using (E4) and (E5),

$$g^{[N-1]}(s) = \frac{(2s+1)(N-1)!}{k!(N-k)!} = \frac{N-2k}{N} \binom{N}{k}. \quad (\text{E8})$$

Therefore

$$\frac{g^{[N-1]}(s) s(s+1)}{2s+1} = \frac{1}{N} \binom{N}{k} s(s+1) = \frac{1}{4N} \binom{N}{k} [(N-2k)^2 - 1], \quad (\text{E9})$$

by (E6).

d. *Step 4: Massaging F_{corr} into final form from (52).* Insert (E7) and (E9) into (E2) and sum over k :

$$\begin{aligned} F_{\text{corr}} &= \frac{N}{2^{2N-2}} \sum_{k=0}^N \frac{1}{3} \left(\frac{1}{4N} \binom{N}{k} [(N-2k)^2 - 1] \right) \cdot 2^N \left(\frac{1}{\sqrt{k+1}} - \frac{1}{\sqrt{N-k+1}} \right)^2 \\ &= \boxed{\frac{1}{3} \cdot \frac{1}{2^N} \sum_{k=0}^N \binom{N}{k} [(N-2k)^2 - 1] \left(\frac{1}{\sqrt{k+1}} - \frac{1}{\sqrt{N-k+1}} \right)^2}. \end{aligned} \quad (\text{E10})$$

Dependence $F_{\text{corr}} = F_{\text{corr}}(N)$ is depicted in Figure 5 showing its non-monotonicity for small values of N .

Now, we move to prove the asymptotic behaviour of F_{corr} , used in the discussion presented below eq. 52 in the main text. We have the following statement:

Lemma 1. *Let*

$$F_{\text{corr}}(N) = \frac{1}{3} \frac{1}{2^N} \sum_{k=0}^N \binom{N}{k} [(N-2k)^2 - 1] \left(\frac{1}{\sqrt{k+1}} - \frac{1}{\sqrt{N-k+1}} \right)^2. \quad (\text{E11})$$

Then, as $N \rightarrow \infty$,

$$F_{\text{corr}}(N) = \frac{2}{N} + O\left(\frac{1}{N^2}\right), \quad \text{in particular} \quad \lim_{N \rightarrow \infty} F_{\text{corr}}(N) = 0. \quad (\text{E12})$$

Proof. Introduce a binomial random variable $K \sim \text{Bin}(N, \frac{1}{2})$. Since $\frac{1}{2^N} \sum_{k=0}^N \binom{N}{k} (\cdot) = \mathbb{E}[(\cdot)]$, we may rewrite

$$F_{\text{corr}}(N) = \frac{1}{3} \mathbb{E}([(N-2K)^2 - 1] \Delta(K)^2), \quad \Delta(K) := \frac{1}{\sqrt{K+1}} - \frac{1}{\sqrt{N-K+1}}.$$

Set $X := K - \frac{N}{2}$, so that $N - 2K = -2X$ and $(N - 2K)^2 - 1 = 4X^2 - 1$. The binomial measure concentrates on K close to $N/2$, i.e. on $|X| = O(\sqrt{N})$, and on this typical set $\Delta(K)$ admits a simple Taylor expansion.

Define $g(t) := (t+1)^{-1/2}$ and note that $\Delta(K) = g(\frac{N}{2} + X) - g(\frac{N}{2} - X)$. By the mean value theorem, there exists a point ξ between $\frac{N}{2} - |X|$ and $\frac{N}{2} + |X|$ such that

$$\Delta(K) = 2X g'(\xi), \quad g'(t) = -\frac{1}{2(t+1)^{3/2}}.$$

On the typical event $A := \{|X| \leq N/4\}$ we have $\xi = \frac{N}{2} + \mathcal{O}(|X|)$ and therefore

$$g'(\xi) = -\frac{1}{2(\frac{N}{2} + 1)^{3/2}} + \mathcal{O}\left(\frac{|X|}{N^{5/2}}\right),$$

which yields

$$\Delta(K)^2 = \frac{X^2}{(\frac{N}{2} + 1)^3} + \mathcal{O}\left(\frac{|X|^3}{N^4}\right) = \frac{8X^2}{N^3} + \mathcal{O}\left(\frac{|X|^3}{N^4}\right).$$

At the same time, the binomial tails are exponentially small, e.g. by a Chernoff bound $\mathbb{P}(A^c) \leq 2e^{-cN}$ for some $c > 0$. Since the integrand in the definition of $F_{\text{corr}}(N)$ grows at most polynomially in N , the contribution of A^c to the expectation is $\mathcal{O}(e^{-cN})$ and hence negligible compared to any inverse power of N .

Consequently, we may evaluate the expectation using the above expansion on A . Multiplying out gives

$$(4X^2 - 1)\Delta(K)^2 = (4X^2 - 1)\left(\frac{8X^2}{N^3} + \mathcal{O}\left(\frac{|X|^3}{N^4}\right)\right) = \frac{32X^4}{N^3} - \frac{8X^2}{N^3} + \mathcal{O}\left(\frac{|X|^5}{N^4}\right).$$

Taking expectations and using the standard central moments of the binomial distribution at $p = \frac{1}{2}$,

$$\mathbb{E}[X^2] = \frac{N}{4}, \quad \mathbb{E}[X^4] = 3\left(\frac{N}{4}\right)^2 - \frac{N}{8} = \frac{3N^2}{16} - \frac{N}{8}, \quad \mathbb{E}[|X|^5] = \mathcal{O}(N^{5/2}),$$

we obtain

$$\mathbb{E}[(4X^2 - 1)\Delta(K)^2] = \frac{32}{N^3} \left(\frac{3N^2}{16} - \frac{N}{8}\right) - \frac{8}{N^3} \cdot \frac{N}{4} + \mathcal{O}\left(\frac{N^{5/2}}{N^4}\right) = \frac{6}{N} + \mathcal{O}\left(\frac{1}{N^2}\right).$$

Finally, multiplying by the prefactor $1/3$, we obtain expressions in (E12). This finishes the proof. \square

Appendix F: Comparison with [31]

Every quantum channel $\mathcal{N} : \mathcal{L}(\mathcal{H}) \rightarrow \mathcal{L}(\mathcal{H})$ admits the Kraus decomposition $\mathcal{N}(\cdot) = \sum_i K_i(\cdot)K_i^\dagger$, where the Kraus operators K_i , satisfy condition $\sum_i K_i^\dagger K_i = \mathbf{1}$. If the channel \mathcal{N} is unital, we have additionally $\sum_i K_i K_i^\dagger = \mathbf{1}$.

For every operator $X \in \mathcal{L}(\mathcal{H})$ and the maximally entangled state $|\psi_{AB}^+\rangle = (1/\sqrt{d}) \sum_i |ii\rangle$, we have so called 'ping-pong' trick:

$$(\mathbf{1}_A \otimes X_B)|\psi_{AB}^+\rangle = (X_A^T \otimes \mathbf{1}_B)|\psi_{AB}^+\rangle, \quad (\text{F1})$$

where T denotes the transposition operation with respect to the local base.

Now, for simplicity, let us consider the action of $\mathcal{E}_{\vec{p}} \otimes \mathcal{E}_{\vec{p}}$ on just one maximally entangled state $P_{AB}^+ := |\psi_{AB}^+\rangle\langle\psi_{AB}^+|$ using the Kraus decomposition:

$$\begin{aligned} (\mathcal{E}_{\vec{p}} \otimes \mathcal{E}_{\vec{p}})P_{AB}^+ &= \sum_{m,n} (K_m \otimes K_n)P_{AB}^+(K_m^\dagger \otimes K_n^\dagger) \\ &= (\mathbf{1} \otimes K_n)(K_m \otimes \mathbf{1})P_{AB}^+(K_m^\dagger \otimes \mathbf{1})(\mathbf{1} \otimes K_n^\dagger) \\ &= \sum_{m,n} (\mathbf{1} \otimes K_n K_m^T)P_{AB}^+(\mathbf{1} \otimes \bar{K}_m K_n^\dagger), \end{aligned} \quad (\text{F2})$$

where the bar denotes complex conjugation. Let us denote by D the number of Kraus operators representing the channel $\mathcal{E}_{\vec{p}}$. Introducing two sets $S := \{1, 2, \dots, D\}$, and $S' := \{1, 2, \dots, D^2\}$, we define a function $f : S \times S \rightarrow S'$, which maps any pair $(m, n) \in S \times S$ to $l \in S'$. This allows us to associate with every term $K_n K_m^T$ another operator, let us call it K_l . The operators K_l are again Kraus operators. Indeed, we have:

$$\begin{aligned} \sum_l K_l^\dagger K_l &= \sum_{m,n} (\bar{K}_m K_n^\dagger)(K_n K_m^T) \\ &= \sum_m \bar{K}_m K_m^T = \sum_m (K_m K_m^\dagger)^T \\ &= \mathbb{1}, \end{aligned} \tag{F3}$$

where in the last equality we use the fact that the Pauli channel is a unital channel. The above calculations show that instead of considering the action of $\mathcal{E}_{\vec{p}} \otimes \mathcal{E}_{\vec{p}}$, it is enough to consider the action of a channel $\tilde{\mathcal{E}}_{\vec{p}}(\cdot) = \sum_l K_l(\cdot) K_l^\dagger$ on the system B only. What is more, the resulting channel $\tilde{\mathcal{E}}_{\vec{p}}$ is again a Pauli channel, but with different parameter \vec{p}' depending on \vec{p} . The explicit relations can be derived having known forms of the Kraus operators for $\mathcal{E}_{\vec{p}}$. It means that their approach can be reduced to studying noisy resource state, where the noise is applied only on the Bob's side.

In our case, the noise is produced by the resource-environment interaction given by the unitary:

$$U_{A_k B_k : E} = \sum_{i,j} |ij\rangle\langle ij|_{A_k B_k} \otimes w_{ij}^E, \tag{F4}$$

where $\{w_{ij}^E\}$ are unitaries. Now, let us consider the initial state for system and environment to be of the form $\rho_{A_k B_k : E} = |\Psi^-\rangle\langle\Psi^-|_{A_k B_k} \otimes \rho_E$. The corresponding channel is

$$\mathcal{C}(\rho_{A_k B_k}) = \text{tr}_E U_{A_k B_k : E} (\rho_{A_k B_k : E}) U_{A_k B_k : E}^\dagger \tag{F5}$$

$$= \frac{1}{2} \sum_{i,j} (-1)^{i+j} \text{tr} \{ w_{j,j \oplus 1}^\dagger w_{i,i \oplus 1} \rho_E \} |i, i \oplus 1\rangle\langle j, j \oplus 1| \tag{F6}$$

$$= \frac{1}{2} \sum_{i,j} |i\rangle\langle j| \otimes \Gamma_{ij} |i \oplus 1\rangle\langle j \oplus 1|. \tag{F7}$$

Here, $\Gamma_{00} = \Gamma_{11} = 1$ and $\Gamma_{01} = \Gamma_{10}^*$. We take $\Gamma_{01} = \Gamma e^{-i\theta}$. Eq. (14) can be expressed as

$$\mathcal{C}(\rho_{A_k B_k}) = \frac{1 + |\Gamma|}{2} \mathbb{1} \otimes R(\theta) |\Psi^-\rangle\langle\Psi^-| \mathbb{1} \otimes R(\theta)^\dagger \tag{F8}$$

$$+ \frac{1 - |\Gamma|}{2} \mathbb{1} \otimes \sigma_z R(\theta) |\Psi^-\rangle\langle\Psi^-| \mathbb{1} \otimes R(\theta)^\dagger \sigma_z^\dagger \tag{F9}$$

$$= \mathbb{1} \otimes \mathcal{E}_{\Gamma, \theta} (|\Psi^-\rangle\langle\Psi^-|). \tag{F10}$$

Here, $\mathcal{E}_{\Gamma, \theta} = \sum_{k=0,1} E_k(\cdot) E_k^\dagger$ is a single qubit Pauli channel with Kraus operators

$$E_0 = \sqrt{\frac{1 + |\Gamma|}{2}} R(\theta) \tag{F11}$$

$$E_1 = \sqrt{\frac{1 - |\Gamma|}{2}} \sigma_z R(\theta), \tag{F12}$$

where $R(\theta)$ is given by Eq. (19).

Let $\tilde{\Psi}_{\vec{B} \vec{A}}$ be the resource state. We can write

$$\tilde{\Psi}_{\vec{B} \vec{A}} = \bigotimes_j^N \tilde{\Psi}_{B_j A_j} = \bigotimes_j^N \mathcal{E}_{\Gamma, \theta} (|\Psi^-\rangle\langle\Psi^-|), \tag{F13}$$

where

$$\begin{aligned} \mathcal{E}_{\Gamma, \theta} (|\Psi^-\rangle\langle\Psi^-|_{B_j A_j}) &= \frac{1 + |\Gamma|}{2} (\mathbb{1} \otimes R(-\theta)) |\Psi^-\rangle\langle\Psi^-|_{B_j A_j} (\mathbb{1} \otimes R(-\theta)^\dagger) \\ &\quad + \frac{1 - |\Gamma|}{2} (\mathbb{1} \otimes \sigma_3 R(-\theta)) |\Psi^-\rangle\langle\Psi^-|_{B_j A_j} (\mathbb{1} \otimes R(-\theta)^\dagger \sigma_3) \end{aligned} \tag{F14}$$

The PBT channel is written as

$$\begin{aligned}\mathcal{C}(\rho_C) &= \sum_{j=1}^N \text{tr}_{\bar{B}_j \bar{A}C} \left[\left(\mathbb{1}_{\bar{B}} \otimes \Pi_{\bar{A}C}^{(j)} \right) \left(\tilde{\Psi}_{\bar{B}\bar{A}} \otimes \rho_C \right) \right] \\ &= \sum_{j=1}^N \text{tr}_{\bar{A}C} \left[\left(\mathbb{1}_{B_j} \otimes \Pi_{\bar{A}C}^{(j)} \right) \left(\text{tr}_{\bar{B}_j} \tilde{\Psi}_{\bar{B}\bar{A}} \otimes \rho_C \right) \right]\end{aligned}\quad (\text{F15})$$

Since $\text{tr}_{\bar{B}_j} \tilde{\Psi}_{\bar{B}\bar{A}} = \tilde{\Psi}_{B_j A_j} \otimes \frac{\mathbb{1}_{\bar{A}_j}}{2^{N-1}}$, we can re-write Eq. (F15) using as

$$\begin{aligned}\mathcal{C}(\rho_C) &= \frac{1+|\Gamma|}{2} \sum_{j=1}^N \text{tr}_{\bar{A}C} \left[\left(\mathbb{1}_{B_j} \otimes \Pi_{\bar{A}C}^{(j)} \right) \left(\left(R(\theta) \otimes \mathbb{1} \left| \Psi^- \right\rangle \left\langle \Psi^- \right|_{B_j A_j} R(\theta)^\dagger \otimes \mathbb{1} \right) \otimes \frac{\mathbb{1}_{\bar{A}_j}}{2^{N-1}} \otimes \rho_C \right) \right] \\ &\quad + \frac{1-|\Gamma|}{2} \sum_{j=1}^N \text{tr}_{\bar{A}C} \left[\left(\mathbb{1}_{B_j} \otimes \Pi_{\bar{A}C}^{(j)} \right) \left(\left(\sigma_3 R(\theta) \otimes \mathbb{1} \left| \Psi^- \right\rangle \left\langle \Psi^- \right|_{B_j A_j} R(\theta)^\dagger \sigma_3 \otimes \mathbb{1} \right) \otimes \frac{\mathbb{1}_{\bar{A}_j}}{2^{N-1}} \otimes \rho_C \right) \right] \\ &= \frac{1+|\Gamma|}{2} R(\theta) \sum_{j=1}^N \text{tr}_{\bar{A}C} \left[\left(\mathbb{1}_{B_j} \otimes \Pi_{\bar{A}C}^{(j)} \right) \left(\left| \Psi^- \right\rangle \left\langle \Psi^- \right|_{B_j A_j} \otimes \frac{\mathbb{1}_{\bar{A}_j}}{2^{N-1}} \otimes \rho_C \right) \right]_{B_j \rightarrow B} R(\theta)^\dagger \\ &\quad + \frac{1-|\Gamma|}{2} \sigma_3 R(\theta) \sum_{j=1}^N \text{tr}_{\bar{A}C} \left[\left(\mathbb{1}_{B_j} \otimes \Pi_{\bar{A}C}^{(j)} \right) \left(\left| \Psi^- \right\rangle \left\langle \Psi^- \right|_{B_j A_j} \otimes \frac{\mathbb{1}_{\bar{A}_j}}{2^{N-1}} \otimes \rho_C \right) \right]_{B_j \rightarrow B} R(\theta)^\dagger \sigma_3 \\ &= \frac{1+|\Gamma|}{2} R(\theta) \mathcal{C}(\rho_C) R(\theta)^\dagger + \frac{1-|\Gamma|}{2} \sigma_3 R(\theta) \mathcal{C}(\rho_C) R(\theta)^\dagger \sigma_3\end{aligned}\quad (\text{F16})$$

Let us consider the case $\theta = 0$. Then

$$\mathcal{C}(\rho_C) = \frac{1+|\Gamma|}{2} \mathcal{C}(\rho_C) + \frac{1-|\Gamma|}{2} \sigma_3 \mathcal{C}(\rho_C) \sigma_3 \quad (\text{F17})$$

Comparing the above channel with Eq. (36) of Kim *et. al.*, we get $\alpha^1 = 0$; $\alpha^2 = 0$ and

$$\begin{aligned}\frac{\alpha^0}{16} &= \frac{1+|\Gamma|}{2} \Rightarrow \alpha^0 = 8(1+|\Gamma|) \\ \frac{\alpha^3}{16} &= \frac{1-|\Gamma|}{2} \Rightarrow \alpha^3 = 8(1-|\Gamma|)\end{aligned}\quad (\text{F18})$$

The corresponding Pauli probabilities are calculated using Eq. (34) of Kim *et. al.* as

$$p_0 = 2(1 + \sqrt{\Gamma}), \quad p_1 = 0, \quad p_2 = 0, \quad p_3 = 2(1 - \sqrt{\Gamma}). \quad (\text{F19})$$

Further, following Eq.(37), we calculate

$$\begin{aligned}q_{\vec{p}} &= \frac{1}{3}((1-p_3)^2 + 2) - \frac{1}{6}p_3^2 \\ &= \frac{1+2\Gamma}{6}\end{aligned}\quad (\text{F20})$$

Since the fidelity for noiseless resource should be equal to Ishizaka *et. al.* for SRM, using $q_{\vec{p}} = 1$ and

$$F = \frac{1}{4} + \frac{3}{4}q_N q_{\vec{p}}, \quad (\text{F21})$$

we get

$$q_N = \frac{4F_{IH} - 1}{3} \quad (\text{F22})$$

Using Eqs. (F20) and (F21),

$$F = \frac{2\Gamma + 1}{3} F_{IH} + \frac{1-\Gamma}{6} \quad (\text{F23})$$

The entanglement fidelity is not the same as our noiseless case in Eq. (50).

Appendix G: Spin–boson model and microscopic origin of the decoherence factor

In this Appendix we provide a microscopic justification of the effective decoherence parameter used in Sec. VII. We remind here that our goal is not to re-derive the port-based teleportation protocol from first principles, but to demonstrate how the single complex decoherence factor

$$\Gamma(t, r) = |\Gamma(t, r)| e^{i\theta(t, r)} \quad (\text{G1})$$

naturally arises from a standard spin–boson model for two spatially separated qubits. Throughout we follow the field-theoretic treatment of dephasing noise in which the separation enters through spatial bath correlations (see, e.g., Ref. [45]).

We consider two qubits forming a Bell pair, located at spatial positions \mathbf{r}_A and \mathbf{r}_B , interacting with a bosonic environment described by

$$H_E = \sum_{\mathbf{k}} \omega_{\mathbf{k}} b_{\mathbf{k}}^\dagger b_{\mathbf{k}}. \quad (\text{G2})$$

The total Hamiltonian of the composite system is therefore given by

$$H = H_S + H_E + H_{\text{int}}, \quad (\text{G3})$$

where H_S denotes the free Hamiltonian of the two qubits. We assume $[H_S, H_{\text{int}}] = 0$, so that the interaction induces pure dephasing without energy exchange.

The interaction Hamiltonian is taken in the position-dependent (field-theoretic) pure-dephasing form

$$H_{\text{int}} = \sum_{\alpha=A,B} \sigma_z^{(\alpha)} \otimes \sum_{\mathbf{k}} \left(g_{\mathbf{k}} e^{i\mathbf{k} \cdot \mathbf{r}_\alpha} b_{\mathbf{k}}^\dagger + g_{\mathbf{k}}^* e^{-i\mathbf{k} \cdot \mathbf{r}_\alpha} b_{\mathbf{k}} \right), \quad (\text{G4})$$

Due to the spatial separation

$$r = |\mathbf{r}_A - \mathbf{r}_B|, \quad (\text{G5})$$

bath-induced correlations are not instantaneous. In the field-theoretic model, the distance dependence enters through phase factors $e^{i\mathbf{k} \cdot (\mathbf{r}_A - \mathbf{r}_B)}$ and, for an isotropic environment with linear dispersion $\omega = ck$, reduces to oscillatory correlation factors $\cos(\omega r/c)$ and $\sin(\omega r/c)$ (see Ref. [45]).

In a multi-qubit spin–boson model, different off-diagonal elements of the reduced density matrix generally decay with different decoherence exponents, depending on the corresponding eigenvalues of the system–bath coupling operator. In the present work we are interested specifically in the coherence relevant for the Bell pair $|\Psi^-\rangle = (|01\rangle - |10\rangle)/\sqrt{2}$, which serves as the elementary entanglement resource in the port-based teleportation protocol. Consequently, the effective decoherence factor entering our description corresponds to the decay of the coherence between the computational basis states $|01\rangle$ and $|10\rangle$.

Within the field-theoretic formulation of collective dephasing, such two-qubit coherences can be expressed in terms of bath correlation functions $\Gamma_{mn}(t)$ [45]. For the $|01\rangle \leftrightarrow |10\rangle$ coherence, the relevant contribution is given by the difference of local and nonlocal bath correlations, which reflects the fact that both basis states acquire identical bath-induced phases in the limit of perfectly correlated noise. As a result, the singlet state belongs to a decoherence-free subspace for vanishing separation between the qubits, while finite separation leads to a nontrivial, distance-dependent decay of the Bell-pair coherence.

Tracing out the bosonic environment yields an effective dephasing of the Bell pair fully characterized by the single complex number $\Gamma(t, r)$. For the Bell-pair coherence relevant to teleportation (equivalently, the coherence between $|01\rangle$ and $|10\rangle$ in the computational basis), one obtains [45]

$$\chi(t, r) = 2 \int_0^\infty d\omega \frac{J(\omega)}{\omega^2} (1 - \cos \omega t) \coth\left(\frac{\beta\omega}{2}\right) [1 - \cos(\omega r/c)], \quad (\text{G6})$$

$$\theta(t, r) = \frac{1}{2} \int_0^\infty d\omega \frac{J(\omega)}{\omega^2} (1 - \cos \omega t) \sin(\omega r/c), \quad (\text{G7})$$

where $J(\omega)$ denotes the spectral density of the environment and $\beta = 1/T$ is the inverse temperature. The decoherence factor reads

$$\Gamma(t, r) = \exp[-\chi(t, r) + i\theta(t, r)], \quad |\Gamma(t, r)| = e^{-\chi(t, r)}. \quad (\text{G8})$$

To make the connection between microscopic bath parameters and the effective decoherence factor more explicit, we consider a generalized Ohmic spectral density with an exponential cutoff,

$$J(\omega) = \frac{\omega^s}{\Lambda^{s-1}} e^{-\omega/\Lambda}. \quad (\text{G9})$$

We introduce dimensionless variables

$$\tilde{\omega} = \frac{\omega}{\Lambda}, \quad \tau = t\Lambda, \quad \vartheta = \frac{T}{\Lambda}, \quad \ell = \frac{r\Lambda}{c}. \quad (\text{G10})$$

In terms of these variables, Eqs. (G6)–(G7) become

$$\chi(\tau, \ell) = 2 \int_0^\infty d\tilde{\omega} \tilde{\omega}^{s-2} e^{-\tilde{\omega}} (1 - \cos(\tilde{\omega}\tau)) \coth\left(\frac{\tilde{\omega}}{2\vartheta}\right) [1 - \cos(\tilde{\omega}\ell)], \quad (\text{G11})$$

$$\theta(\tau, \ell) = \frac{1}{2} \int_0^\infty d\tilde{\omega} \tilde{\omega}^{s-2} e^{-\tilde{\omega}} (1 - \cos(\tilde{\omega}\tau)) \sin(\tilde{\omega}\ell), \quad (\text{G12})$$

and the decoherence factor can be written as

$$\Gamma(\tau, \ell) = \exp[-\chi(\tau, \ell) + i\theta(\tau, \ell)], \quad |\Gamma(\tau, \ell)| = e^{-\chi(\tau, \ell)}. \quad (\text{G13})$$

This shows explicitly that all microscopic bath properties and the finite separation enter the teleportation protocol solely through the single complex parameter $\Gamma(\tau, \ell)$.

Derivation of Eqs. (H6)–(H7) from Tuziemski Eqs. (17)–(20)

We start from the multi-qubit pure-dephasing (spin–boson) model as in Tuziemski *et al.* [45], where the reduced dynamics of the register coherences can be written in terms of bath correlation matrices $\Gamma(t)$, $\Gamma^\pm(t)$. In particular, Tuziemski writes the (complex) decoherence factor between two register basis states $|\epsilon\rangle$ and $|\epsilon'\rangle$ ($\epsilon_n, \epsilon'_n \in \{\pm\frac{1}{2}\}$ being the eigenvalues of $J_z^{(n)} = \frac{1}{2}\sigma_z^{(n)}$) as [45, Eq. (15)]

$$-\log \gamma_{\epsilon\epsilon'}(t) = \Delta\epsilon^T \Gamma(t) \Delta\epsilon + i\left(\epsilon^T \Gamma^+(t) \epsilon - \epsilon'^T \Gamma^+(t) \epsilon' - 2\epsilon^T \Gamma^-(t) \epsilon'\right), \quad \Delta\epsilon := \epsilon - \epsilon'. \quad (\text{G14})$$

The matrices entering (G14) are specified by Tuziemski via a position-dependent coupling vector

$$\mathbf{g}_\mathbf{k} = g_\mathbf{k}(e^{-i\mathbf{k}\cdot\mathbf{r}_1}, e^{-i\mathbf{k}\cdot\mathbf{r}_2}), \quad (\text{G15})$$

and the mode-sum definitions [45, Eqs. (18)–(20)]

$$\Gamma_{nm}(t) = \frac{1}{2} \sum_{\mathbf{k}} |g_{\mathbf{k}} \alpha_{\mathbf{k}}(t)|^2 \coth\left(\frac{\omega_{\mathbf{k}}}{2k_B T}\right) \cos(\mathbf{k} \cdot (\mathbf{r}_n - \mathbf{r}_m)), \quad (\text{G16})$$

$$\Gamma_{nm}^+(t) = \sum_{\mathbf{k}} |g_{\mathbf{k}}|^2 \xi_{\mathbf{k}}(t) \cos(\mathbf{k} \cdot (\mathbf{r}_n - \mathbf{r}_m)), \quad (\text{G17})$$

$$\Gamma_{nm}^-(t) = \frac{1}{2} \sum_{\mathbf{k}} |g_{\mathbf{k}} \alpha_{\mathbf{k}}(t)|^2 \sin(\mathbf{k} \cdot (\mathbf{r}_n - \mathbf{r}_m)). \quad (\text{G18})$$

Here, we have used $\mathbf{r}_1 \equiv \mathbf{r}_A$ and $\mathbf{r}_2 \equiv \mathbf{r}_B$ for inconvenience. To obtain the final expressions from the previous paragraph, we need to execute the following steps:

Identify the relevant coherence. In NPBT we need the coherence between the two-qubit computational basis

states $|01\rangle$ and $|10\rangle$, since it controls the singlet Bell component. We place the qubits at \mathbf{r}_A and \mathbf{r}_B and define $r := |\mathbf{r}_A - \mathbf{r}_B|$. With the convention $\sigma_z |0\rangle = +|0\rangle$ and $\sigma_z |1\rangle = -|1\rangle$, the $J_z = \frac{1}{2}\sigma_z$ eigenvalue strings are

$$\epsilon(|01\rangle) = \left(+\frac{1}{2}, -\frac{1}{2} \right), \quad \epsilon'(|10\rangle) = \left(-\frac{1}{2}, +\frac{1}{2} \right), \quad \Delta\epsilon = (1, -1). \quad (\text{G19})$$

Real part (decay exponent) in terms of $\Gamma_{nm}(t)$. For two qubits the matrix $\Gamma(t)$ is symmetric and has equal diagonals, $\Gamma_{11}(t) = \Gamma_{22}(t)$, and $\Gamma_{12}(t) = \Gamma_{21}(t)$. Thus,

$$\begin{aligned} \Delta\epsilon^T \Gamma(t) \Delta\epsilon &= (1, -1) \begin{pmatrix} \Gamma_{11}(t) & \Gamma_{12}(t) \\ \Gamma_{12}(t) & \Gamma_{11}(t) \end{pmatrix} \begin{pmatrix} 1 \\ -1 \end{pmatrix} \\ &= \Gamma_{11}(t) - 2\Gamma_{12}(t) = 2(\Gamma_{11}(t) - \Gamma_{12}(t)). \end{aligned} \quad (\text{G20})$$

Therefore, the modulus decay of the $|01\rangle \langle 10|$ coherence is governed by $\Gamma_{11}(t) - \Gamma_{12}(t)$. Similarly,

$$\begin{aligned} \epsilon^T \Gamma^+(t) \epsilon &= \frac{1}{4}(1, -1) \begin{pmatrix} \Gamma_{11}^+(t) & \Gamma_{12}^+(t) \\ \Gamma_{12}^+(t) & \Gamma_{11}^+(t) \end{pmatrix} \begin{pmatrix} 1 \\ -1 \end{pmatrix} \\ &= \frac{1}{4} [\Gamma_{11}^+(t) + \Gamma_{22}^+(t) - (\Gamma_{12}^+(t) + \Gamma_{21}^+(t))] = \frac{1}{2}(\Gamma_{11}^+(t) - \Gamma_{12}^+(t)), \end{aligned} \quad (\text{G21})$$

$$\begin{aligned} \epsilon'^T \Gamma^+(t) \epsilon' &= \frac{1}{4}(-1, 1) \begin{pmatrix} \Gamma_{11}^+(t) & \Gamma_{12}^+(t) \\ \Gamma_{12}^+(t) & \Gamma_{11}^+(t) \end{pmatrix} \begin{pmatrix} -1 \\ 1 \end{pmatrix} \\ &= \frac{1}{4} [\Gamma_{11}^+(t) + \Gamma_{22}^+(t) - (\Gamma_{12}^+(t) + \Gamma_{21}^+(t))] = \frac{1}{2}(\Gamma_{11}^+(t) - \Gamma_{12}^+(t)), \end{aligned} \quad (\text{G22})$$

and

$$\begin{aligned} \epsilon^T \Gamma^-(t) \epsilon' &= \frac{1}{4}(1, -1) \begin{pmatrix} \Gamma_{11}^-(t) & \Gamma_{12}^-(t) \\ \Gamma_{12}^-(t) & \Gamma_{11}^-(t) \end{pmatrix} \begin{pmatrix} -1 \\ 1 \end{pmatrix} \\ &= -\frac{1}{4} [\Gamma_{11}^-(t) + \Gamma_{22}^-(t) - (\Gamma_{12}^-(t) + \Gamma_{21}^-(t))] = \frac{1}{2}\Gamma_{12}^-(t). \end{aligned} \quad (\text{G23})$$

Here, we have used $\Gamma_{11}^+(t) = \Gamma_{22}^+(t)$, $\Gamma_{12}^+(t) = \Gamma_{21}^+(t)$, $\Gamma_{11}^-(t) = \Gamma_{22}^-(t) = 0$ and $\Gamma_{12}^-(t) = \Gamma_{21}^-(t)$ followed from (G17) and (G18)

Turn the mode sums into spectral-density integrals. The standard interaction-picture displacement amplitude is $\alpha_{\mathbf{k}}(t) = (1 - e^{i\omega_{\mathbf{k}}t})/\omega_{\mathbf{k}}$, so that

$$|\alpha_{\mathbf{k}}(t)|^2 = \frac{2(1 - \cos\omega_{\mathbf{k}}t)}{\omega_{\mathbf{k}}^2}. \quad (\text{G24})$$

Inserting (G24) into (G16) gives

$$\Gamma_{nm}(t) = \sum_{\mathbf{k}} |g_{\mathbf{k}}|^2 \frac{1 - \cos(\omega_{\mathbf{k}}t)}{\omega_{\mathbf{k}}^2} \coth\left(\frac{\omega_{\mathbf{k}}}{2k_B T}\right) \cos(\mathbf{k} \cdot (\mathbf{r}_n - \mathbf{r}_m)). \quad (\text{G25})$$

Passing to the continuum limit and introducing the spectral density $J(\omega) = \sum_{\mathbf{k}} |g_{\mathbf{k}}|^2 \delta(\omega - \omega_{\mathbf{k}})$ yields

$$\Gamma_{nm}(t) = \int_0^\infty d\omega J(\omega) \frac{1 - \cos(\omega t)}{\omega^2} \coth\left(\frac{\omega}{2k_B T}\right) \cos(\omega \tau_{nm}), \quad \tau_{nm} := \frac{|\mathbf{r}_n - \mathbf{r}_m|}{c}, \quad (\text{G26})$$

in agreement with Tuziemski's continuum expressions [45, Eq. (27)]. Similarly,

$$\Gamma_{nm}^-(t) = \frac{1}{2} \int_0^\infty d\omega J(\omega) \frac{1 - \cos(\omega t)}{\omega^2} \sin(\omega \tau_{nm}). \quad (\text{G27})$$

For the two-qubit case, $\tau_{11} = 0$ and $\tau_{12} = r/c$, and hence,

$$\Delta\epsilon^T \Gamma(t) \Delta\epsilon = 2 \int_0^\infty d\omega J(\omega) \frac{1 - \cos(\omega t)}{\omega^2} \coth\left(\frac{\omega}{2k_B T}\right) (1 - \cos(\omega r/c)), \quad (\text{G28})$$

and

$$\boldsymbol{\epsilon}^T \Gamma^-(t) \boldsymbol{\epsilon}' = \frac{1}{4} \int_0^\infty d\omega J(\omega) \frac{1 - \cos(\omega t)}{\omega^2} \sin(\omega r/c), \quad (\text{G29})$$

Combining (G14), and (G21)-(G23)

$$-\log \gamma_{\epsilon\epsilon'}(t) = \Delta \boldsymbol{\epsilon}^T \Gamma(t) \Delta \boldsymbol{\epsilon} - 2i \boldsymbol{\epsilon}^T \Gamma^-(t) \boldsymbol{\epsilon}' \quad (\text{G30})$$

Comparing (G30) with (G8), and using (G28) and (G29) for spectral forms, $\chi(t, r)$ and $\theta(t, r)$ are expressed as

$$\chi(t, r) = 2 \int_0^\infty d\omega \frac{J(\omega)}{\omega^2} (1 - \cos(\omega t)) \coth\left(\frac{\beta\omega}{2}\right) (1 - \cos(\omega r/c)) \quad (\text{G31})$$

$$\theta(t, r) = \frac{1}{2} \int_0^\infty d\omega \frac{J(\omega)}{\omega^2} (1 - \cos(\omega t)) \sin(\omega r/c). \quad (\text{G32})$$

[1] S. Ishizaka and T. Hiroshima, Asymptotic Teleportation Scheme as a Universal Programmable Quantum Processor, *Physical Review Letters* **101**, 240501 (2008).

[2] S. Ishizaka and T. Hiroshima, Quantum teleportation scheme by selecting one of multiple output ports, *Physical Review A* **79**, 042306 (2009).

[3] C. H. Bennett, G. Brassard, C. Crépeau, R. Jozsa, A. Peres, and W. K. Wootters, Teleporting an unknown quantum state via dual classical and Einstein-Podolsky-Rosen channels, *Physical Review Letters* **70**, 1895 (1993).

[4] M. A. Nielsen and I. L. Chuang, Programmable quantum gate arrays, *Phys. Rev. Lett.* **79**, 321 (1997).

[5] Y. Yang, R. Renner, and G. Chiribella, Optimal universal programming of unitary gates, *Phys. Rev. Lett.* **125**, 210501 (2020).

[6] M. Studziński, S. Strelchuk, M. Mozrzymas, and M. Horodecki, Port-based teleportation in arbitrary dimension, *Scientific Reports* **7**, 10871 (2017), arXiv:1612.09260 [quant-ph].

[7] M. Mozrzymas, M. Studziński, S. Strelchuk, and M. Horodecki, Optimal port-based teleportation, *New Journal of Physics* **20**, 053006 (2018), arXiv:1707.08456 [quant-ph].

[8] Z.-W. Wang and S. L. Braunstein, Higher-dimensional performance of port-based teleportation, *Scientific Reports* **6**, 33004 (2016).

[9] M. Christandl, F. Leditzky, C. Majenz, G. Smith, F. Speelman, and M. Walter, Asymptotic performance of port-based teleportation, *Communications in Mathematical Physics* 10.1007/s00220-020-03884-0 (2020).

[10] F. Leditzky, Optimality of the pretty good measurement for port-based teleportation, *Letters in Mathematical Physics* **112** (2022).

[11] P. Taranto, S. Milz, M. Murao, M. T. Quintino, and K. Modi, Higher-order quantum operations (2025), arXiv:2503.09693 [quant-ph].

[12] J. Pereira, L. Banchi, and S. Pirandola, Characterising port-based teleportation as universal simulator of qubit channels, *Journal of Physics A: Mathematical and Theoretical* **54**, 205301 (2021).

[13] G. Muguruza and F. Speelman, Port-Based State Preparation and Applications, *Quantum* **8**, 1573 (2024).

[14] V. Bržić, S. Yoshida, M. Murao, and M. T. Quintino, Higher-order quantum computing with known input states (2025), arXiv:2510.20530 [quant-ph].

[15] S. Yoshida, Y. Koizumi, M. Studziński, M. T. Quintino, and M. Murao, One-to-one correspondence between deterministic port-based teleportation and unitary estimation (2024), arXiv:2408.11902 [quant-ph].

[16] M. T. Quintino, Q. Dong, A. Shimbo, A. Soeda, and M. Murao, Reversing unknown quantum transformations: Universal quantum circuit for inverting general unitary operations, *Phys. Rev. Lett.* **123**, 210502 (2019).

[17] M. T. Quintino, Q. Dong, A. Shimbo, A. Soeda, and M. Murao, Probabilistic exact universal quantum circuits for transforming unitary operations, *Phys. Rev. A* **100**, 062339 (2019).

[18] M. T. Quintino and D. Ebler, Deterministic transformations between unitary operations: Exponential advantage with adaptive quantum circuits and the power of indefinite causality, *Quantum* **6**, 679 (2022).

[19] M. Sedláček, A. Bisio, and M. Ziman, Optimal Probabilistic Storage and Retrieval of Unitary Channels, *Phys. Rev. Lett.* **122**, 170502 (2019), arXiv:1809.04552 [quant-ph].

[20] A. Bisio, G. Chiribella, G. M. D'Ariano, S. Facchini, and P. Perinotti, Optimal quantum learning of a unitary transformation, *Phys. Rev. A* **81**, 032324 (2010).

[21] S. Beigi and R. König, Simplified instantaneous non-local quantum computation with applications to position-based cryptography, *New Journal of Physics* **13**, 093036 (2011).

[22] A. May, Complexity and entanglement in non-local computation and holography, *Quantum* **6**, 864 (2022).

[23] H. Buhrman, L. Czekaj, A. Grudka, M. Horodecki, P. Horodecki, M. Markiewicz, F. Speelman, and S. Strelchuk, Quantum communication complexity advantage implies violation of a Bell inequality, *Proceedings of the National Academy of Sciences* **113**, 3191 (2016).

- [24] J. L. Pereira, L. Banchi, and S. Pirandola, Continuous variable port-based teleportation, arXiv:2302.08522 (2023).
- [25] S. Pirandola, R. Laurenza, C. Lupo, and J. L. Pereira, Fundamental limits to quantum channel discrimination, *npj Quantum Information* **5**, 50 (2019), arXiv:1803.02834 [quant-ph].
- [26] E. Chitambar and F. Leditzky, On the duality of teleportation and dense coding, *IEEE Transactions on Information Theory* **70**, 3529 (2024).
- [27] D. Grinko, A. Burchardt, and M. Ozols, Gelfand-tsetlin basis for partially transposed permutations, with applications to quantum information (2023), arXiv:2310.02252 [quant-ph].
- [28] J. Fei, S. Timmerman, and P. Hayden, Efficient quantum algorithm for port-based teleportation (2023), arXiv:2310.01637 [quant-ph].
- [29] D. Grinko, A. Burchardt, and M. Ozols, Efficient quantum circuits for port-based teleportation (2024), arXiv:2312.03188 [quant-ph].
- [30] A. Wills, M.-H. Hsieh, and S. Strelchuk, Efficient algorithms for all port-based teleportation protocols, *PRX Quantum* **5**, 030354 (2024).
- [31] H. E. Kim and K. Jeong, Port-based entanglement teleportation via noisy resource states, *Physica Scripta* **99**, 035105 (2024).
- [32] G. M. Palma, K.-a. Suominen, and A. Ekert, Quantum computers and dissipation, *Proceedings of the Royal Society A: Mathematical, Physical and Engineering Sciences* **452**, 567 (1996), <https://royalsocietypublishing.org/rspa/article-pdf/452/1946/567/998471/rspa.1996.0029.pdf>.
- [33] J. H. Reina, L. Quiroga, and N. F. Johnson, Decoherence of quantum registers, *Phys. Rev. A* **65**, 032326 (2002).
- [34] M. Schlosshauer, *Decoherence: And the Quantum-To-Classical Transition* (Springer, 2007).
- [35] B. Ruggiero, P. Delsing, C. Granata, Y. A. Pashkin, and P. Silvestrini, *Quantum computing in solid state systems* (Springer, New York, NY, 2006).
- [36] A. Predojević and M. Mitchell, *Engineering the Atom-Photon Interaction: Controlling Fundamental Processes with Photons, Atoms and Solids*, Nano-Optics and Nanophotonics (Springer International Publishing, 2015).
- [37] F. Gaitan, *Quantum Error Correction and Fault Tolerant Quantum Computing* (CRC Press, Boca Raton, FL, 2008).
- [38] U. Weiss, *Quantum Dissipative Systems*, 5th ed. (World Scientific Publishing Company, Singapore, 2021).
- [39] M. Horodecki, P. Horodecki, and R. Horodecki, General teleportation channel, singlet fraction, and quasidistillation, *Phys. Rev. A* **60**, 1888 (1999).
- [40] T. Yu and J. H. Eberly, Finite-time disentanglement via spontaneous emission, *Phys. Rev. Lett.* **93**, 140404 (2004).
- [41] W. Dür, C. Simon, and J. I. Cirac, Stability of macroscopic entanglement under decoherence, *Physical Review Letters* **92**, 180403 (2004).
- [42] W. H. Zurek, Decoherence, einselection, and the quantum origins of the classical, *Reviews of Modern Physics* **75**, 715 (2003).
- [43] M. Schlosshauer, Quantum decoherence, *Physics Reports* **831**, 1 (2019), quantum decoherence.
- [44] K. Roszak and J. K. Korbicz, Purifying teleportation, *Quantum* **7**, 923 (2023).
- [45] J. Tuziemski, A. Lampo, M. Lewenstein, and J. K. Korbicz, Decoherence of spin registers revisited, *Physical Review A* **99**, 022122 (2019), arXiv:1811.01808, arXiv:1811.01808 [quant-ph].
- [46] H. Barnum and E. Knill, Reversing quantum dynamics with near-optimal quantum and classical fidelity, *Journal of Mathematical Physics* **43**, 2097 (2002).
- [47] A. Montanaro, A lower bound on the probability of error in quantum state discrimination, in *2008 IEEE Information Theory Workshop* (2008) pp. 378–380.
- [48] K. M. R. Audenaert and M. Mosonyi, Upper bounds on the error probabilities and asymptotic error exponents in quantum multiple state discrimination, *Journal of Mathematical Physics* **55**, 102201 (2014), https://pubs.aip.org/aip/jmp/article-pdf/doi/10.1063/1.4898559/14758713/102201_1_online.pdf.
- [49] C. R. Harris, K. J. Millman, S. J. van der Walt, R. Gommers, P. Virtanen, D. Cournapeau, E. Wieser, J. Taylor, S. Berg, N. J. Smith, *et al.*, Array programming with numpy, *Nature* **585**, 357 (2020).
- [50] Y. C. Eldar, A. Megretski, and G. C. Verghese, Optimal detection of symmetric mixed quantum states, *IEEE Transactions on Information Theory* **50**, 1198 (2004).
- [51] A. Assalini, G. Cariolaro, and G. Pierobon, Efficient optimal minimum error discrimination of symmetric quantum states, *Phys. Rev. A* **81**, 012315 (2010).
- [52] C. W. Helstrom, *Quantum Detection and Estimation Theory* (Academic Press, New York, NY, USA, 1976).